

Project no.:
019809

Project acronym:
NextGenBioWaste

Project title:
Innovative demonstrations for the next generation of biomass and waste combustion plants for energy recovery and renewable electricity production

Instrument: Integrated project

Thematic priority: 6.1.3.1.4

Start date of project: 2006-02-24

Duration: 4 years

D 2.6.26

Comparison of different CFD packages with different fuel bed models (GKS)

Revision [draft]

Due date of deliverable: 2010-02-19
Actual submission date: yyyy-mm-dd

Organisation name of lead contractor for this deliverable: GKS

Project co-funded by the European Commission within the Sixth Framework Program (2002-2006)		
Dissemination Level		
PU	Public	X
PP	Restricted to other program participants (including the Commission Services)	
RE	Restricted to a group specified by the consortium (including the Commission Services)	
CO	Confidential , only for members of the consortium (including the Commission Services)	

Deliverable number:	D 2.6.26
Deliverable name:	Comparison of different CFD packages with different fuel bed models
Work package:	WP 2.6 Boiler Optimisation/Design – Demonstration
Lead contractor:	Peter Paul van het Veen

Status of deliverable		
Action	By	Date (yyyy-mm-dd)
Submitted (Author(s))		
Verified (WP-leader)		
Approved (SP-leader)		

Author(s)			
Name	Organisation	E-mail	Tel
Ragnar Warnecke	GKS	Ragnar.warnecke@gks-sw.de	+49(9721)6580-120

Abstract
<p>CFD simulations are an excellent method to investigate engineering and construction. In the present deliverable two plants (AVR and GKS) have been simulated. For the GKS plant several simulations have been compared: on the one hand side the work done by Sintef with an in-house developed CFD-code and on the other hand side by GKS with a commercial code from CFX. The results show an agreement while some differences can be detected. For the different boundary conditions the release of volatiles from the fuel bed is significant. The TNO fuel bed model (TNO-FBM) shows very late reactions of the carbon content, while the GKS fuel bed model (GKS-FBM) has finished the combustion some meters before the grate ends. The different fast and detailed kinetic models (F-KM and D-KM) are not very different. Unfortunately the kinetic model could have been investigated at the GKS plant with the GKS detailed kinetic model only; because the results of a simulation with a detailed kinetic model from Sintef had not been available from Sintef before delivering this report.</p> <p>All in all the results give promising interpretation of the process. Obviously the commercial CFD code is faster to implement whereas the Sintef-code is probably more flexible.</p>

TABLE OF CONTENTS

	Page
1. INTRODUCTION	2
2. SIMULATION OVERVIEW AND BOUNDARY CONDITIONS	3
3. PRESENTATION OF THE DIFFERENT SIMULATIONS	4
3.1 AVR-Symmetry: CFX with TNO-Model and modified fast kinetic Work by TNO	4
3.1.1 Modifications to the model	5
3.1.2 Results.....	6
3.1.3 Conclusions.....	7
3.2 GKS-Symmetry	9
3.2.1 Fuel bed	9
3.2.2 Air inlets	10
3.2.3 Work by Sintef.....	12
3.2.4 Work by GKS	24
4. DISCUSSION	39
4.1 Differences in Simulation Tools.....	39
4.2 Influence of chemistry concept	41
4.3 Influence of concept of bedmodel	43
5. SUMMARY AND OUTLOOK	47
6. LITERATURE	48

1. INTRODUCTION

In former times waste was a source of illness and pestilence. Incineration is the appropriate measure for on the one hands side inertisation of waste to a non-dangerous, hygienic matter and on the other hand minimizing its volume. Waste incineration under controlled conditions in a technical plant is part of the waste handling for more than one hundred years now and seems to be the appropriate technique for the future.

While the combustion of more or less homogenous fossil energy material (i.e. gas, oil, lignite, coal) is investigated extensively in the last decades, the understanding of the combustion process for strongly heterogeneous materials as waste, RDF, biomass etc. is rudimental.

In the plants with heterogeneous fuel a lot of problems can occur: These can be for example the stability of the combustion itself, the release of corrosive species and of deposit causing particles.

- CFD can lead to better understanding of the process
- CFD can help to optimize plants
- Important are the boundary conditions: fuel bed (described in D2.6.25)

2. SIMULATION OVERVIEW AND BOUNDARY CONDITIONS

Within the work package different approaches to the simulation of furnaces are outlined. The most obvious difference is found with the CFD-Codes. ANSYS-CFX is a commercial product, whereas Spider is a proprietary development by Sintef. Within this CFD-Codes the treatment of the reaction-process itself can be done in different ways. The most common are the Eddy Dissipation Model (fast chemistry) and the Eddy-Dissipation-Concept (detailed chemistry). As a third important parameter the generation of the boundary conditions for the simulation is introduced. The so called Fuel-Bed-Model (FBM) is a stand-alone simulation tool which describes the processes in the fuel bed.

Overview over the used tools:

1. CFD-codes:
 - Spider (Sintef)
 - CFX (commercial)

2. Reaction models:
 - Sintef : Eddy Dissipation Model
 - TNO : Modified Eddy Dissipation Model
 - GKS : Eddy Dissipation Model
 - GKS : Eddy-Dissipation-Concept

3. Fuel bed models (see D2.6.25):
 - TNO
 - GKS

4. Number of Cells

Tab. 2-1 Overview of simulations

Plant	Simulation done by	CFD-Code	Fuel-bed-model	Reaction treatment	No cells
AVR	TNO	CFX	TNO	modified fast chemistry	200.000
GKS	Sintef	Spider	TNO	fast chemistry	70.000
GKS	Sintef	Spider	TNO	fast chemistry	180.000
GKS	Sintef	Spider	GKS	fast chemistry	70.000
GKS	GKS	CFX	GKS	fast chemistry	30.000
GKS	GKS	CFX	GKS	detailed chemistry	30.000

3. PRESENTATION OF THE DIFFERENT SIMULATIONS

In following chapter it will be presented 6 simulations. As the AVR plant is done only by TNO, it cannot be compared while the simulations of GKS can be compared with each other.

3.1 AVR-Symmetry: CFX with TNO-Model and modified fast kinetic Work by TNO

TNO work is done on the redesigned furnace 1 of AVR Rozenburg (The Netherlands), where the flue gas flow has been changed from counter-current to co-current flow.

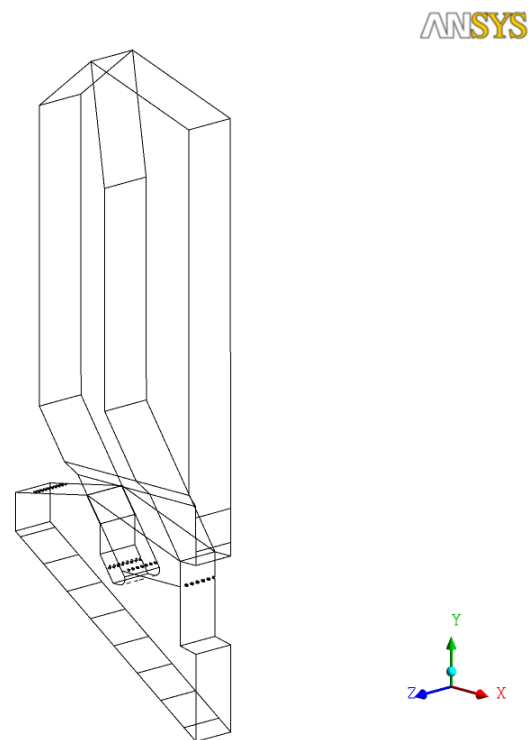
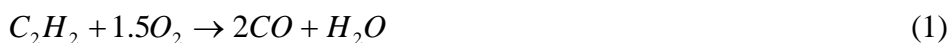


Figure 3.1 Wireframe of 3D model

The fireside of this boiler was modelled using the Computational Fluid Dynamics (CFD) package ANSYS-CFX11.

Five combustion reactions have been applied, for which the Eddy Dissipation Model (EDM) was used.

The oxidation of acetylene runs via a two-step reaction:



Formaldehyde dissociates according to:



Furthermore there are the oxidation reactions:



3.1.1 Modifications to the model

To model combustion in the furnace the Eddy Dissipation Model was used. The empirical coefficient A_{mag} in this model determines the mixing rate. It is proposed to take $A_{mag} = 4.0$, however for simulation of biomass grate furnaces a value of $A_{mag} = 0.6$ should be used [20]. This has been done in the present study as well. Furthermore it appeared that the gasification reaction of the tar component C_2H_2 runs too fast using the EDM model. Hence a combination of the EDM model with the Finite Rate Chemistry (FRC) model has been used. The FRC model is based on the Arrhenius formula. It appeared that the pre-exponential factor in this formula was far too large, as the standard factor for gaseous acetylene was used. Knowing that the tar components consist of long chain molecules and after some calculations with a presumed burnout distance of tar, the value of $2.5E8$ has been decreased to $7.4E4 [s^{-1} mol^{-0.75} m^{2.25}]$.

3.1.2 Results

Two simulations have been performed:

- the design case in which the oxygen in the secondary air has been replaced by nitrogen and
- a second one in which the secondary air is replaced by steam.

Evaluating the results can be done by comparing concentration plots. Figure 3.2 shows the CO mass fractions at three locations in the first draft of the boiler, at heights of 17, 24 and 28 m for the case of secondary air without oxygen.

Secondary air without oxygen

ANSYS

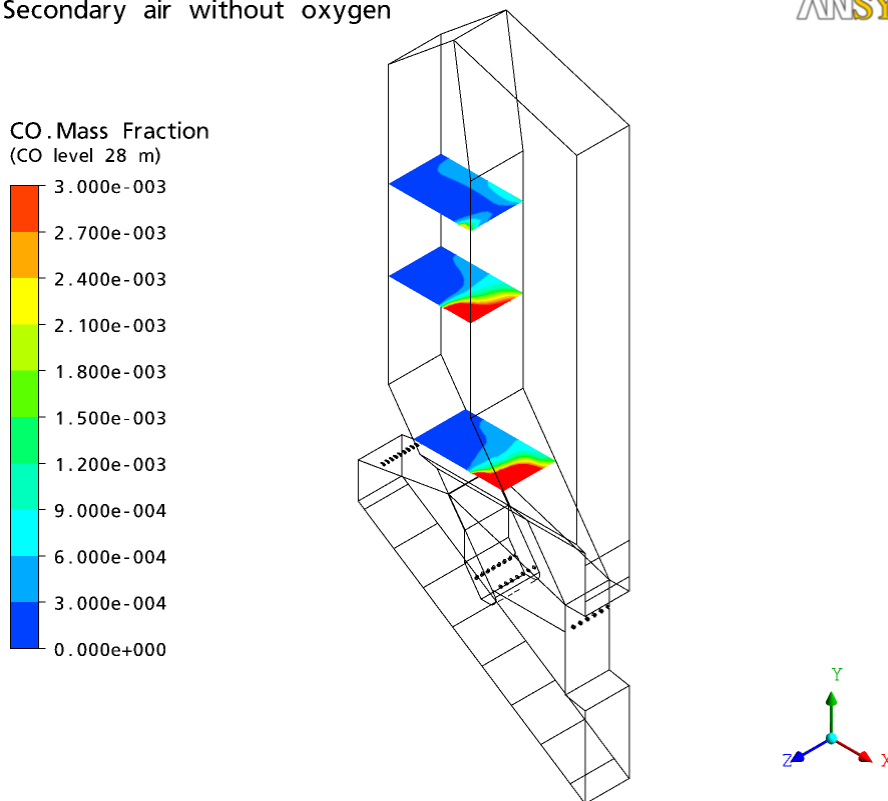


Figure 3.2 CO mass fractions on three levels for secondary flow without O₂

Figure 3.3 is the same plot for the case with injection of steam. It can be seen that the mass fractions in the latter case are lower, but a more quantitative comparison is difficult in this way.

Secondary flow of steam

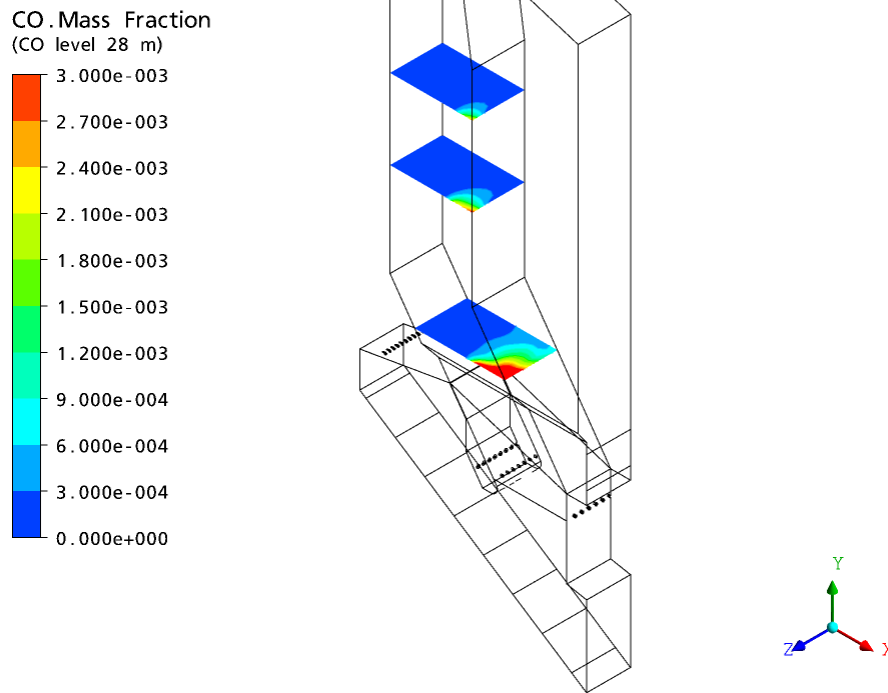


Figure 3.3 CO mass fractions on three levels for secondary flow of steam

It is seen that injection without oxygen yields an increase in CO content at the 17 m level with a factor of about 2.5. Flowing further through the first and second plane the CO contents decreases until a value of 55 mg/Nm^3 is reached at the outlet. That value is barely higher than in the design case. In case of injection with steam it is seen that the CO content at the 17 m level is somewhat higher than in the design case, but the CO is burnt flowing along the planes, until the value at the outlet is 14 mg/Nm^3 . It is clear that mixing is better in case of steam injection. After some analysis it appears that the momentum of the steam injection is higher than in the other case due to the fact that the same mass flow rate has been used (6.46 kg/s at 373 K). As the molecular weight of steam is lower than that of air, the volume rate of the steam is larger, yielding a better mixing.

In both cases it is seen that the oxygen content at the outlet is about 0.55 m%, indicating that the amount of oxygen in the primary air is just enough for combustion.

It can be concluded from these results that a better mixing will certainly improve combustion, but that the CO concentration will increase at least at the beginning of the first draft. Such large CO concentrations could potentially present a problem in causing corrosion. Furthermore one could wonder if the low surplus of oxygen will be sufficient when a sudden rise in CO content takes place. It should also be kept in mind that the standard deviation in the oxygen measurement is 2%, so that reducing the content at the outlet to 0.55% is not under discussion.

3.1.3 Conclusions

It can be concluded from this study that the applied CFD model is capable of predicting the consequences of variations in operating conditions. Lowering the oxygen level appears to be possible provided the mixing is increased through optimised injection of secondary air (with lowered O_2 content) or injection of steam or recirculated flue gas.

Quantitative results of optimization measures cannot be given at this stage of investigation, as it appears that the computational results are (very) sensitive to parameters in the combustion models. There seems to be consensus of opinion on the A_{mag} in the Eddy Dissipation Model, which should have a value of 0.6 in case of biomass combustion. However, the parameters in the Arrhenius equation applied in the Finite Rate Chemistry model are difficult to determine, particularly for the tar component of the fuel represented by C_2H_2 .

3.2 GKS-Symmetry

The GKS-plant was simulated with different CFD-codes, fuel-bed-models and reaction-models. The simulations were done by Sintef and GKS. In Tab. 2-1 the individual simulations are summarized.

3.2.1 Fuel bed

The fuel bed at the bottom of the furnace is modelled based on separate waste layer models, developed by TNO and by GKS.

These models describe the conversion of the waste when travelling along the grate. It includes mass- and energy balances over the height and the length of the bed. The two models are described in NextGenBioWaste deliverable D2.6.26. In the present work these waste layer models are not integrated with the CFD calculations, however the models are used to provide input data for the gas release from the fuel bed.

TNO waste layer model

The model provides the inlet normal speed, temperature, and the mass fractions for the components C, C₂H₂, CH₂O, CO, CO₂, H₂, H₂O, O₂ and N₂. Nitrogen components, the NO_x precursors HCN, NH₃ and NO, are also provided. Figure 3.4 shows mass flows for the different gas components as well as the gas temperatures along the grate provided by the TNO waste layer model. These data describes the fuel release from the GKS grate in the CFD calculations.

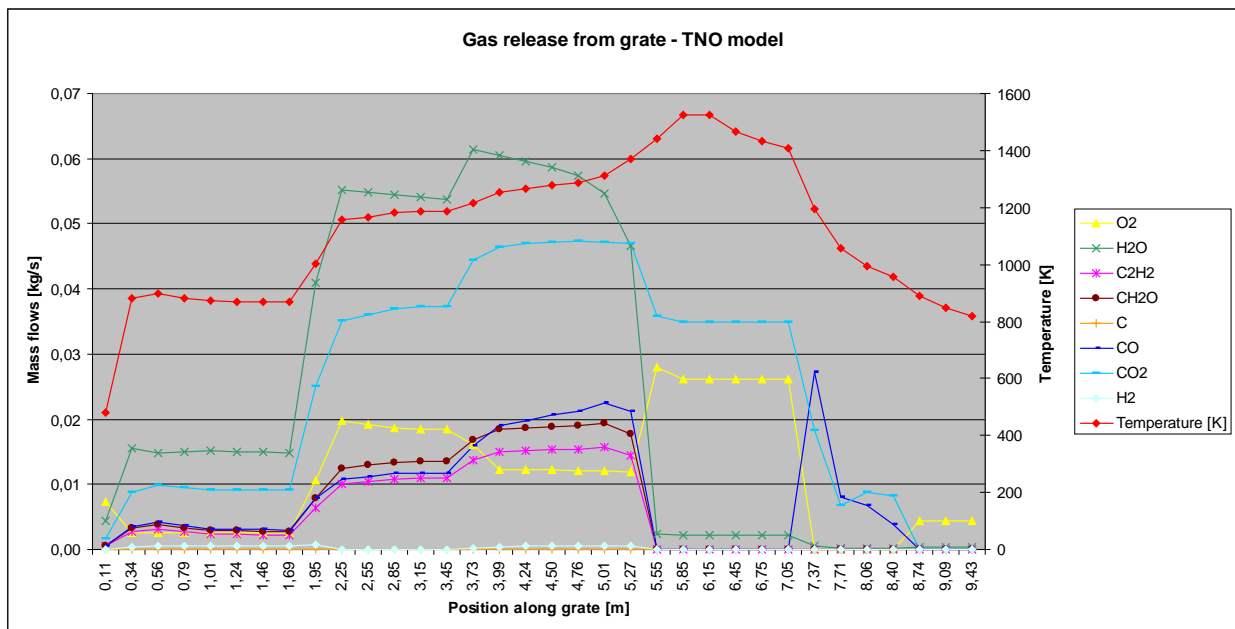


Figure 3.4 Gas release data from the fuel bed provided by the TNO model

GKS waste layer models

The model provides the inlet normal speed, temperature, and the mass fractions for the components C₃H₈, CO, CO₂, H₂, H₂O, O₂ and N₂. Figure 3.5 shows mass flows for the different gas components as well as the gas temperatures along the grate provided by the GKS waste layer model. These data describes the fuel release from the grate in the CFD calculations. The mass

flows Figure 3.4 and Figure 3.5 cannot be compared directly, because the resolution along the grate differs in the two waste layer models, the GKS model has 18 cells along the grate while the TNO model has 34.

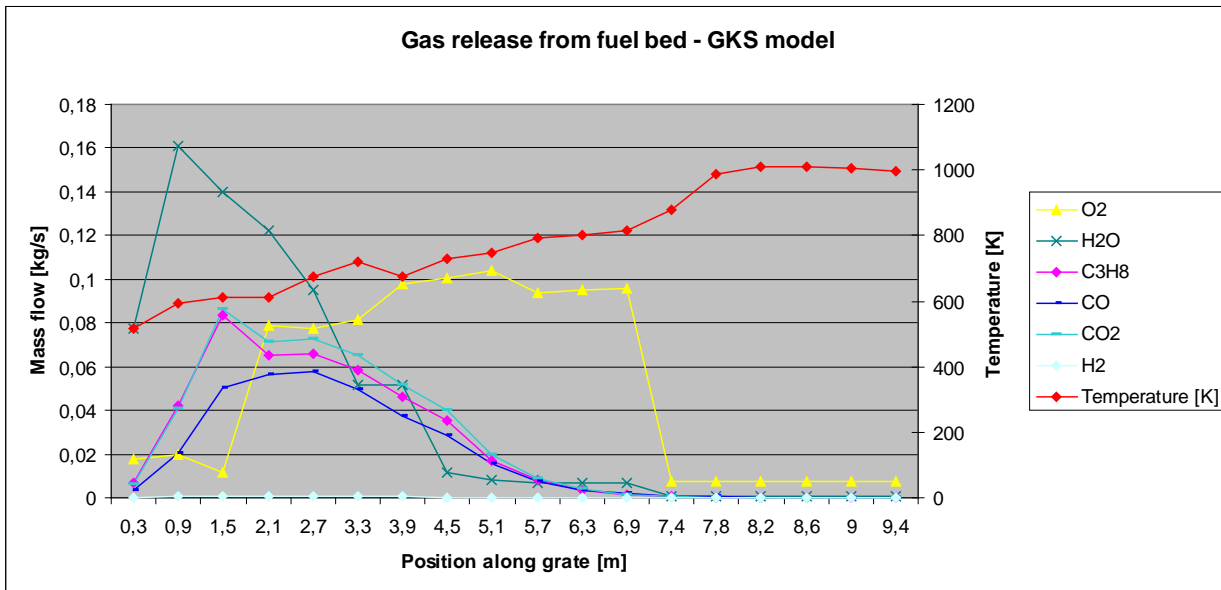


Figure 3.5 Gas release data from the fuel bed provided by the GKS model

3.2.2 Air inlets

The air inlets are based on input received from GKS. The air inlet through the grate (= underfire air) is included in the gas released from the fuel bed.

Specifications received from GKS regarding the air inlets and the rezi nozzles are summarized below:

Side air:

	Flow [Nm ³ /h]	Mass flow [kg/s]	Temperature [°C]	Velocity [m/s]
PL1 one Side	1800	0.6437	120	0.50
PL2 one Side	975	0.3487	120	0.25
PL3 one Side	525	0.1877	120	0.14
PL4 one Side	450	0.1609	120	0.17
Side air both Sides	7500	1.3410	120	

Secondary air

	Mass flow [kg/s]	Temperature [°C]	Velocity [m/s]	Velocity x [m/s]	Velocity y [m/s]
Front wall Nozzle 1 - 6	0.166	120	52.2	52.199	-0.166
Rear wall Nozzle 1-4	0.248	120	78.299	-76.322	-17.483

Rezi nozzles (1-9) at side walls:

Massflow [kg/s]	0.137
Temperature [°C]	150
Velocity [m/s]	61.032

Secondary air

The secondary air is injected through 6 nozzles at one level in the front wall and 4 nozzles at another level in the rear wall, totally 10 nozzles. The nozzles in the rear wall have a higher mass flow than the nozzles in the front wall. The secondary air temperature is 120°C.

In Model 2 the secondary air inlets are resolved such that the velocity is about ½ of the specified. In model 1 the resolution is resulting in a velocity of about 44% of the specified. The mass flow is according to specifications for all inlets for both models.

Side air

Air at 120°C is injected through the side walls just above the grate in four different zones that nearly correspond to zone 1-4 at the grate. The height of the side air inlets is ~0.9m. The side air velocity is quite low, ranging from 0.14 to 0.5 m/s.

Tab. 3-1 Inlet conditions for side air

	Flow [Nm ³ /h]	Mass flow [kg/s]	Temperature [°C]	Velocity [m/s]
PL1 one Side	1800	0.6437	120	0.50
PL2 one Side	975	0.3487	120	0.25
PL3 one Side	525	0.1877	120	0.14
PL4 one Side	450	0.1609	120	0.17
Side air one Side	7500	1.3410	120	

Re-circulated flue gas

Re-circulating flue gas is injected through 9 nozzles at each side wall. The temperature is 150°C. In the calculations, the flue gas composition in the rezi nozzles is based on complete combustion of gases released from the grate (TNO model) with the air flows specified by GKS for side air and secondary air, resulting in the flue gas composition given in Tab. 3-2.

For Model 2 the nozzles with re-circulating flue gas are resolved such that they provide the same velocity and mass flow for all the inlets. The velocity is 21m/s for these inlets which is about 1/3 of the specified velocity. For model 1 the velocity for the re-circulating flue gas is 10-18% of the specified. The mass flow is according to specifications for all inlets in both models.

Tab. 3-2 Inlet conditions for Rezi nozzles (1-9) at side walls

Mass flow [kg/s]	0.137
Temperature [°C]	150
CO ₂ [kg/kg]	0.2032
H ₂ O [kg/kg]	0.1066
O ₂ [kg/kg]	0.0404
N ₂ [kg/kg]	0.6498
Molecular weight [kg/kmole]	28.56

3.2.3 Work by Sintef

3.2.3.1 Numerical tool

SPIDER is a general-purpose CFD (Computational Fluid Dynamics) code, which is based on finite volumes and non-orthogonal curvilinear computational mesh.

3.2.3.2 Physical models

For turbulence the standard high-Reynolds-number $k-\varepsilon$ model with log-law wall function is used.

The interaction between turbulence and combustion is modeled with the Eddy Dissipation Concept (EDC) by Magnussen /3/. In SPIDER, the EDC model can be used with the fast chemistry limit assumption or with a detailed representation of chemical kinetics e.g. with data from a comprehensive reaction mechanism.

The PG98 mechanism /15/ used in the present work contains 65 species and 438 elementary reactions. It is considered as one of the state-of-the-art reaction mechanisms for the prediction of NO_x formation in combustion.

In the waste layer model developed by GKS, propane is defined as the tar component. The PG98 mechanism was extended with propane chemistry from Grimech 3.0 in order to be able to handle propane.

The turbulent combustion calculations with detailed chemistry are designed for parallel calculations on an in-house Linux cluster. The calculations in the present work are run on 64 cpus in parallel.

3.2.3.3 GKS-Symmetry: Geometry

GKS has made available to SINTEF the geometry of the furnace in electronic format (igs-file), and the 3-dimensional geometry model is made based on this. The geometry is symmetric, and the model includes one half of the furnace. A symmetry plane is defined through the longitudinal centre plane of the furnace. The model includes the furnace and the first draft, and the grate is modeled as continuous, without the step. A wire frame of the 3-dimensional model is shown in Figure 3.6.

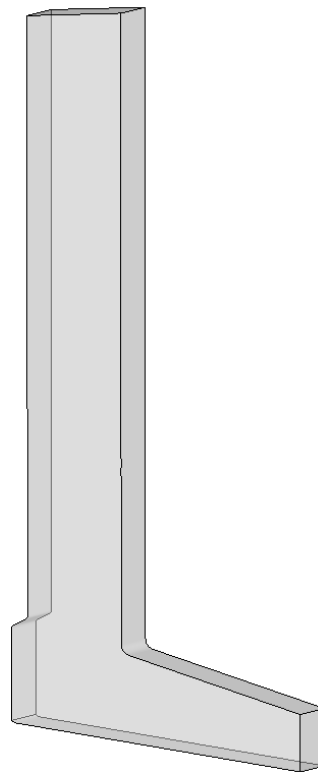


Figure 3.6 Wire frame of the geometry model

SPIDER is a general-purpose CFD code, which is based on finite volumes and non-orthogonal curvilinear computational mesh. The CFD code works with structured mesh. During the present work it has turned out to be challenging to make a satisfactory structured mesh for this specific geometry, and there is put much effort in meshing of the geometry. We have made two different models (mesh).

Geometry 1

This mesh has been created as a simpler model to be used to include and verify the physical models with a relatively short calculation time. The mesh was generated with Gambit, the ANSYS Fluent grid generator, and consists of $30 \times 119 \times 20 = 71.400$ nodes.

The grate is resolved by 34 nodes (Zone 1 - 8, Zone 2 - 6, Zone 3 - 7, Zone 4 - 6, Zone 5 - 7)
 Nodes across the grate (to symmetry plane) - 20
 Nodes above the grate in primary chamber: 30

The nozzles with re-circulating flue gas and the secondary air nozzles are not defined with their specific inlet area, but included as mass sources. The mass flow, gas composition and temperature are according to the specifications, and hence the velocity is dependent of the cross-section area of the specific control volume. The secondary air nozzles are resolved with the same cross-section area, resulting in a velocity of about 44% of the specified. The velocity for the recirculated flue gas is 10-18% of the specified.

The Model 1 mesh of the primary chamber is shown in Figure 3.7.

Geometry 2

The mesh, which consists of 171x51x21=183.141 nodes, has been created to provide better resolution of the geometry and flow field and smoother mesh especially around corners and sharp edges. The Model 2 mesh of the primary chamber is shown in Figure 3.8. An in-house grid generator was used to generate the grid.

The grate is resolved by 42 nodes (compared to 34 in model No1)
 Nodes across the grate (to symmetry plane): 21
 Nodes above the grate in primary chamber: 51

The nozzles with re-circulating flue gas are resolved such that they provide the same velocity and mass flow for all the inlets. The velocity is 21m/s for these inlets which is about 1/3 of the specified velocity. The secondary air inlets are resolved such that the velocity is about 1/2 of the specified. The mass flow is according to specifications for all inlets.

In Geometry 2 the solid walls are specified as isothermal with wall temperature 553K.

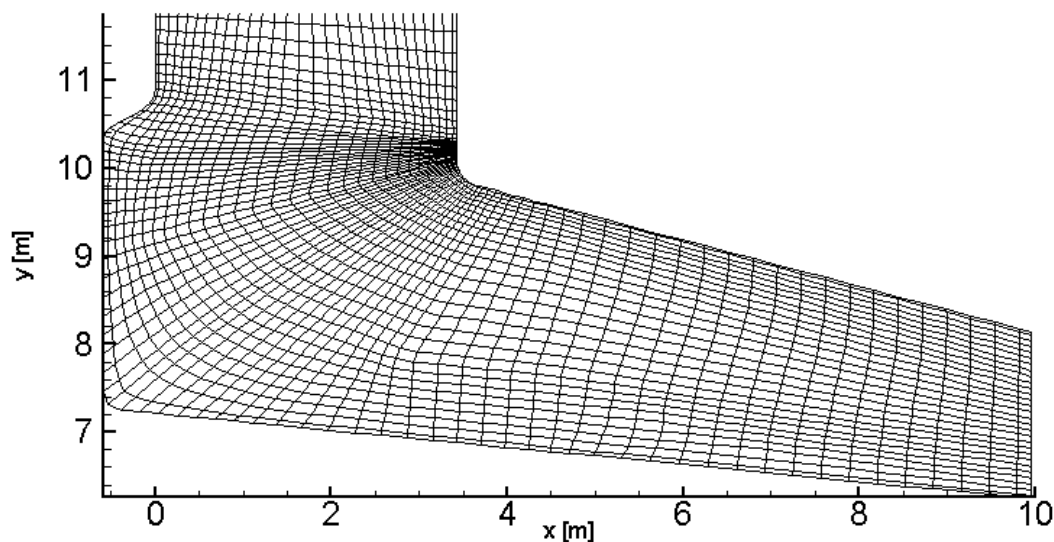


Figure 3.7 Model 1 mesh of primary chamber (the grid lines shown are drawn through the centre points)

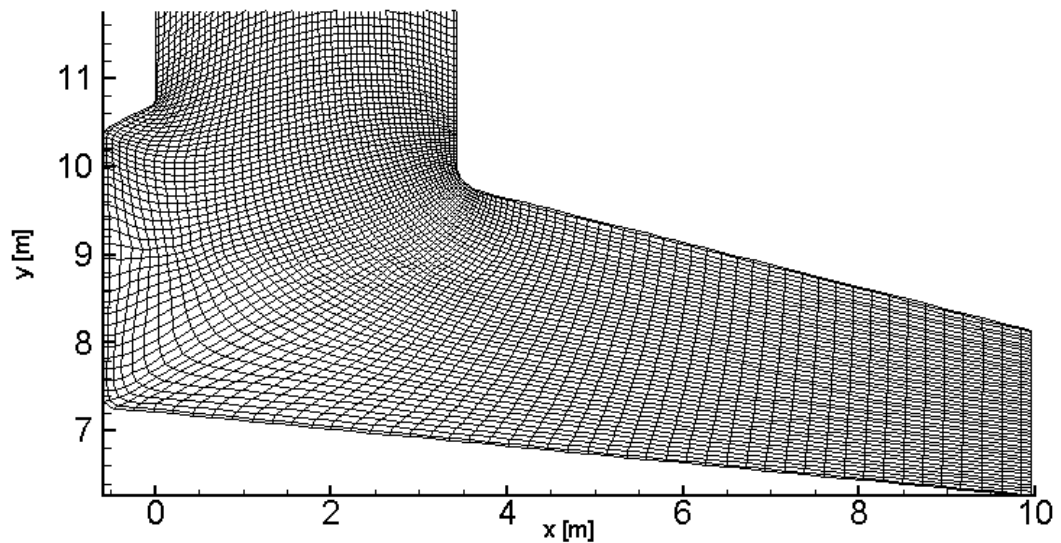


Figure 3.8 Model 2 mesh of primary chamber (the grid lines shown are drawn through the centre points)

3.2.3.4 GKS-Symmetry: Spider with TNO-Model and fast kinetic for Geometry 1

The calculations results for Model No 1 using the TNO waste layer model and the fast chemistry limit assumption for the combustion model (mixed-is-burned mode) are shown in the following Figures. Temperature, CO concentration and oxygen concentration are presented.

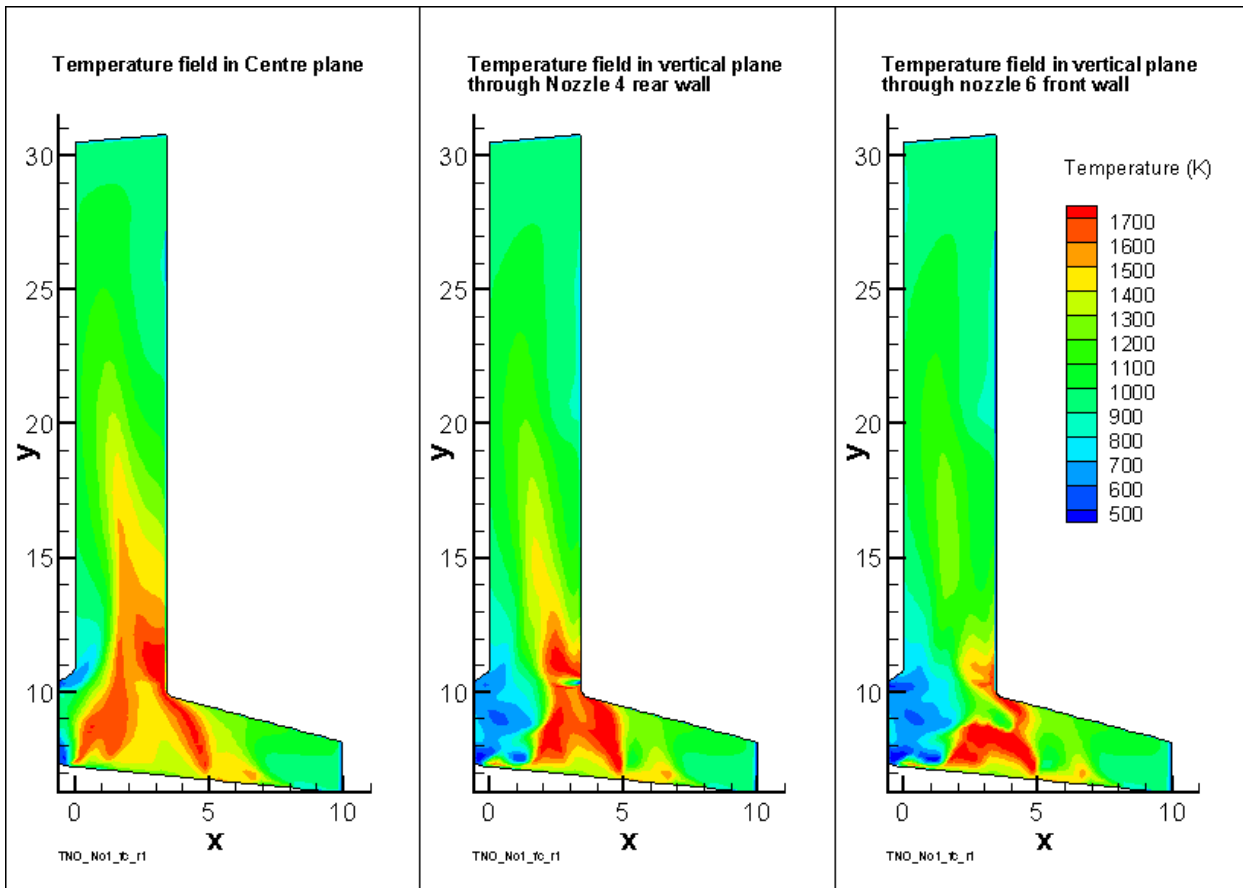


Figure 3.9 Temperature (K) shown in three different vertical planes

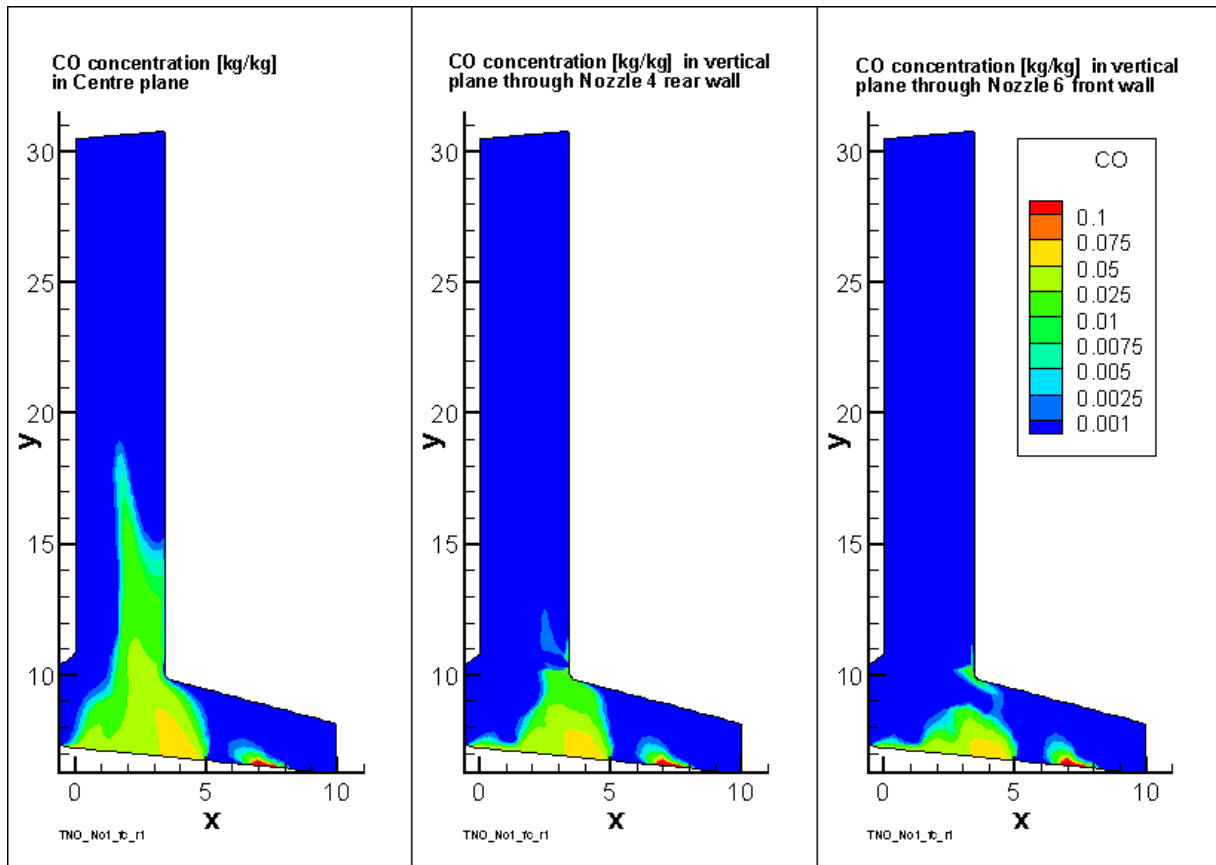


Figure 3.10 CO concentration (kg/kg) shown in three different vertical planes

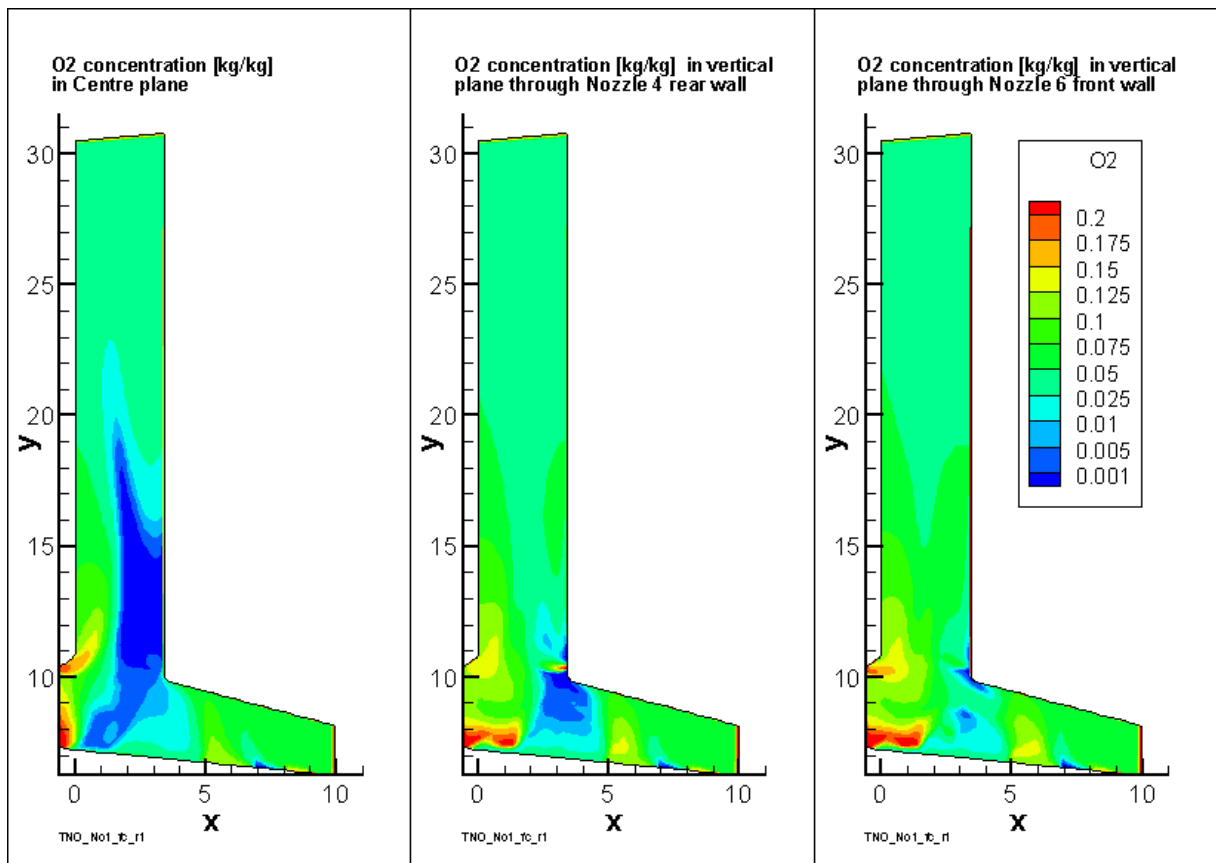


Figure 3.11 Oxygen concentration (kg/kg) shown in three different vertical planes

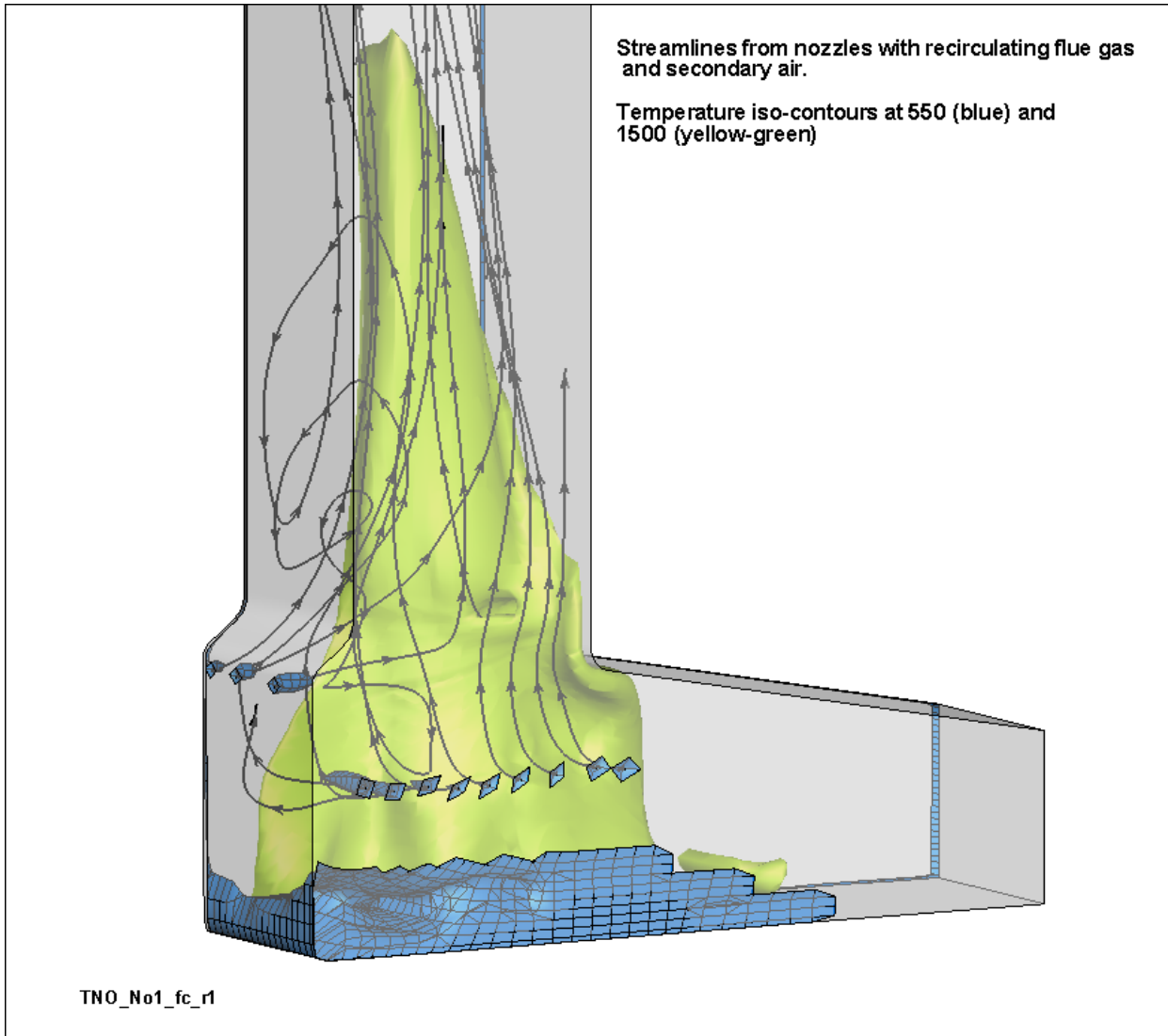


Figure 3.12 Streamlines and iso-surfaces of the temperature

3.2.3.5 GKS-Symmetry: Spider with TNO-Model and fast kinetic for Geometry 2

The calculations results for Model No 2 using the TNO waste layer model and the fast chemistry limit assumption for the combustion model (mixed-is-burned mode) are shown in the following Figures. Temperature, CO concentration and oxygen concentration are presented.

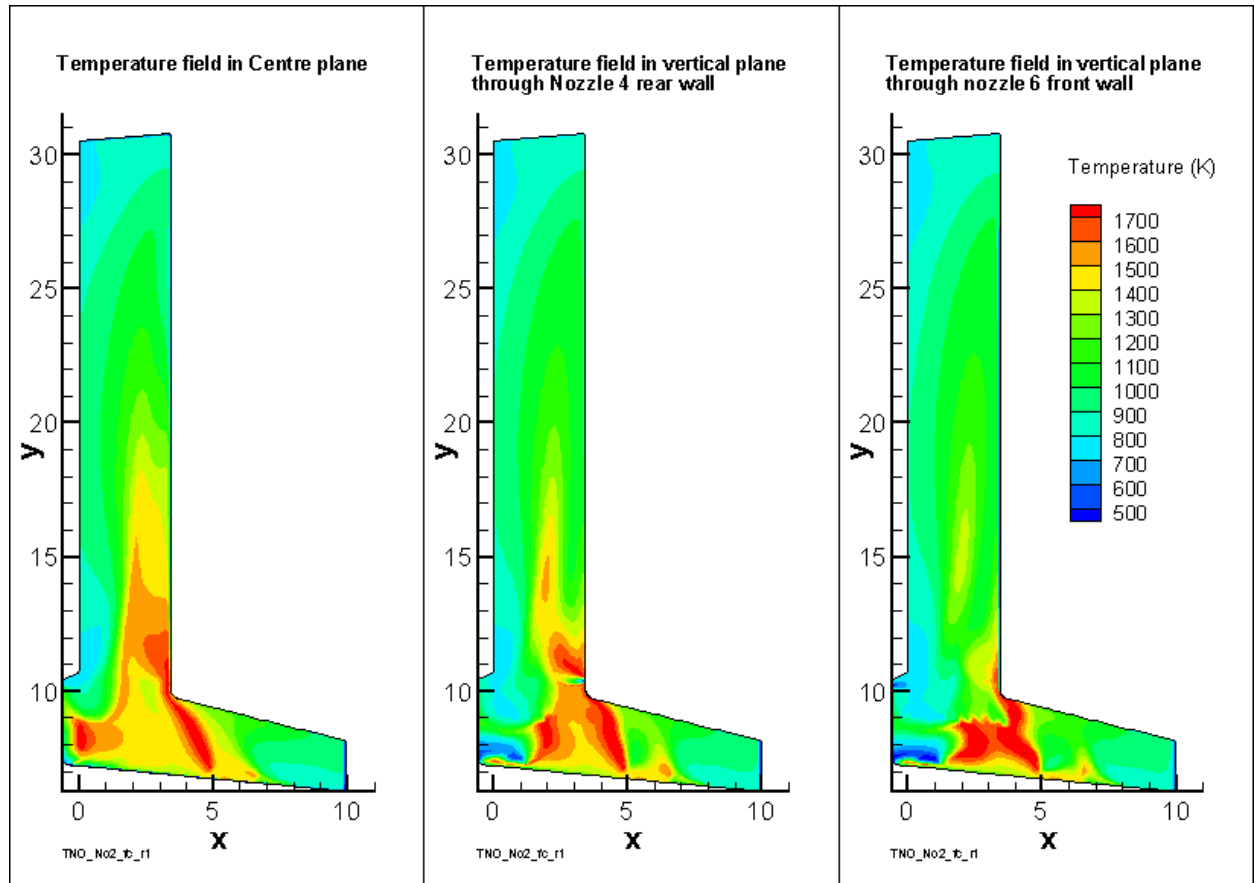


Figure 3.13 Temperature (K) shown in three different vertical planes

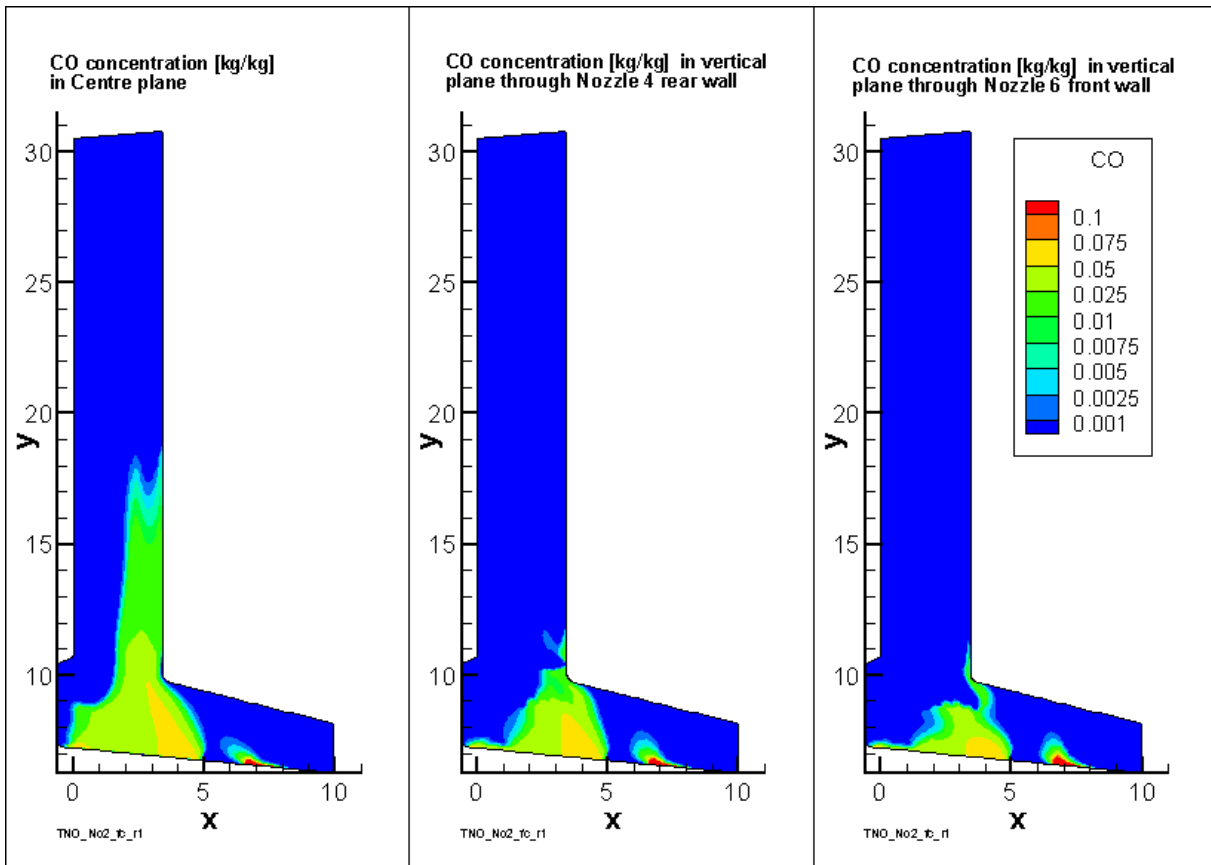


Figure 3.14 CO concentration (kg/kg) shown in three different vertical planes

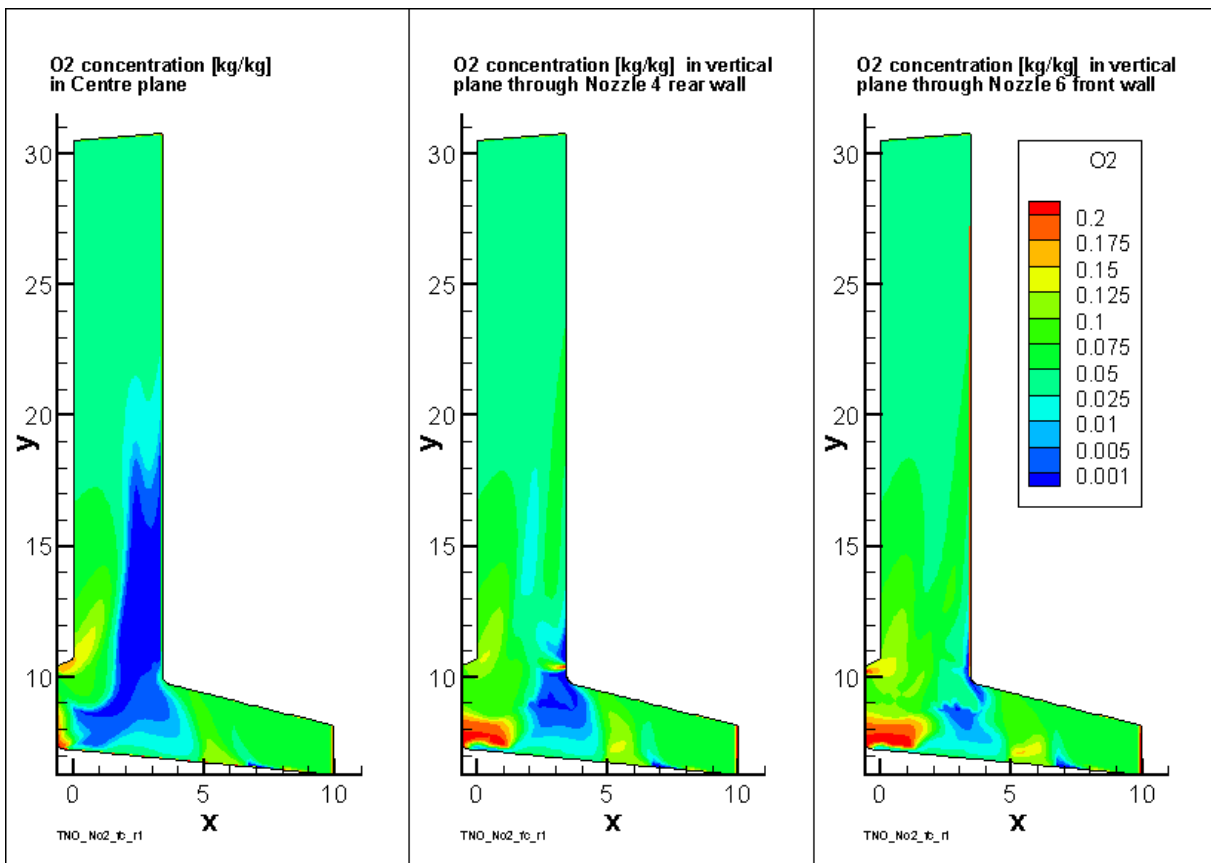


Figure 3.15 Oxygen concentration (kg/kg) shown in three different vertical planes

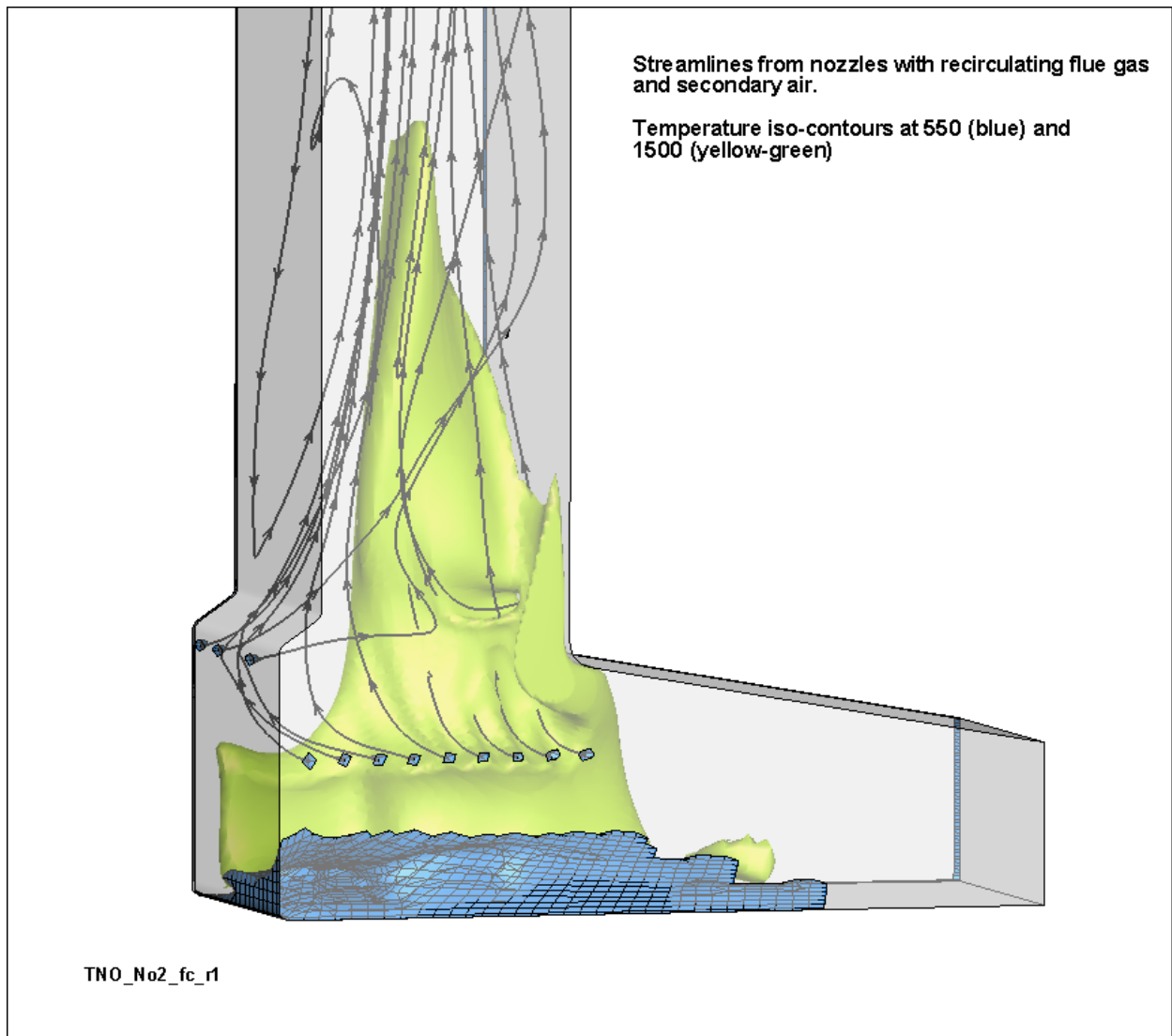


Figure 3.16 Streamlines and isosurfaces

3.2.3.6 GKS-Symmetry: Spider with GKS-Model and fast kinetic

The calculations results for Model No 1 using the GKS waste layer model and the fast chemistry limit assumption for the combustion model (mixed-is-burned mode) are shown in the following Figures. Temperature, CO concentration and oxygen concentration are presented.

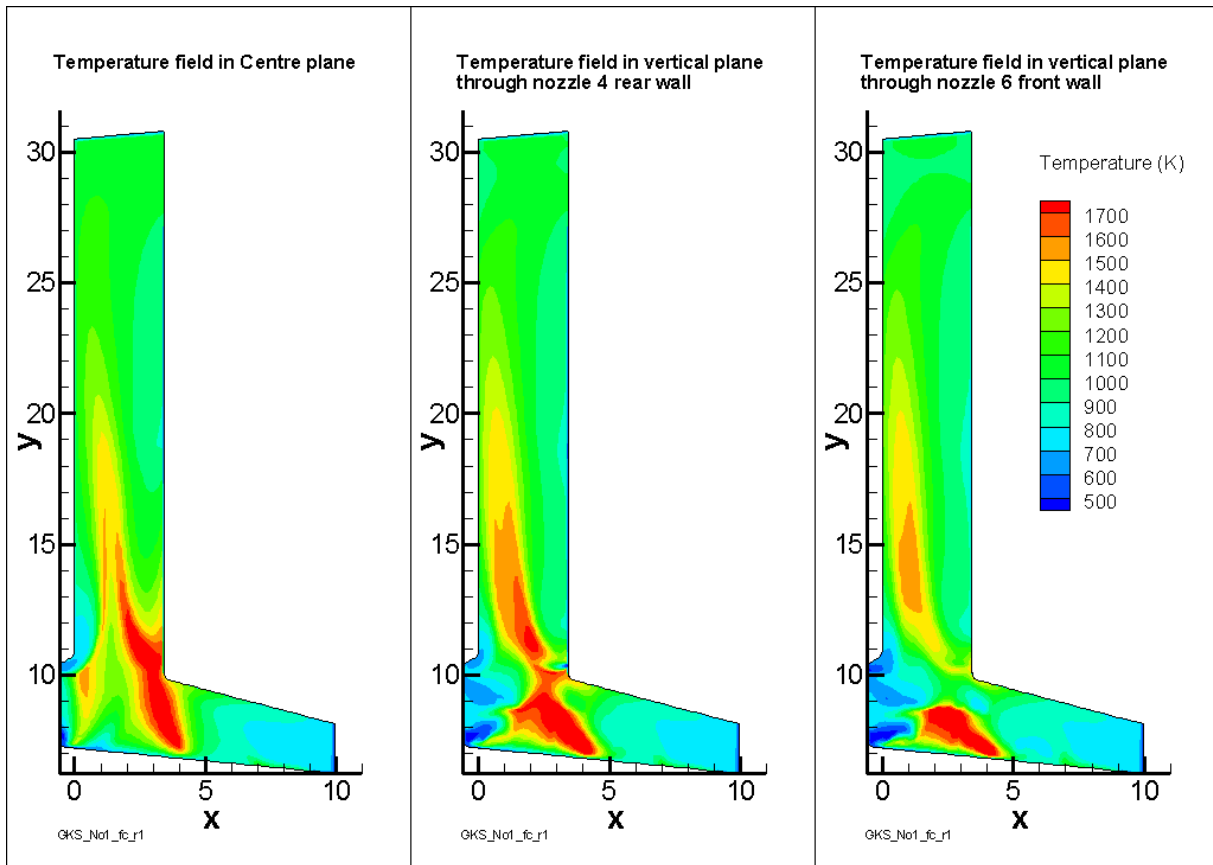


Figure 3.17 Temperature (K) shown in three different vertical planes

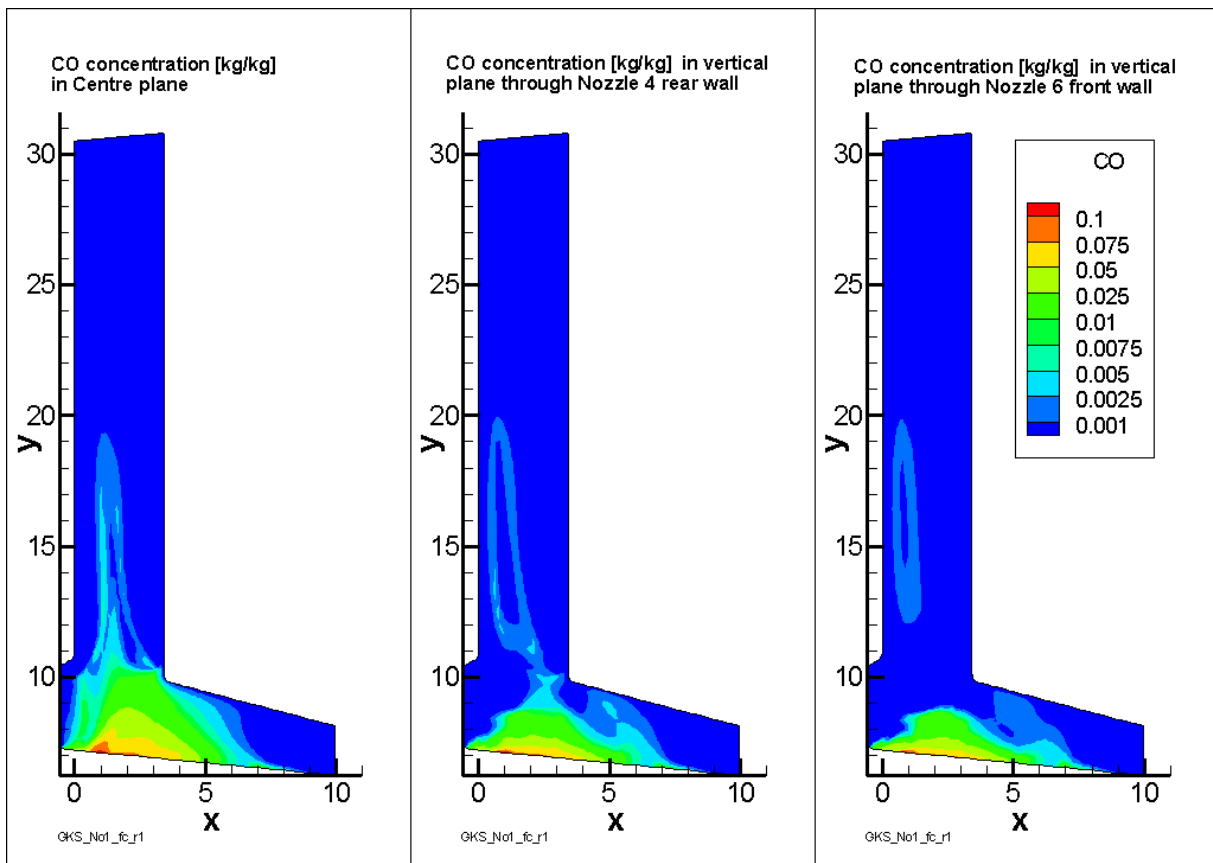


Figure 3.18 CO concentration (kg/kg) shown in three different vertical planes

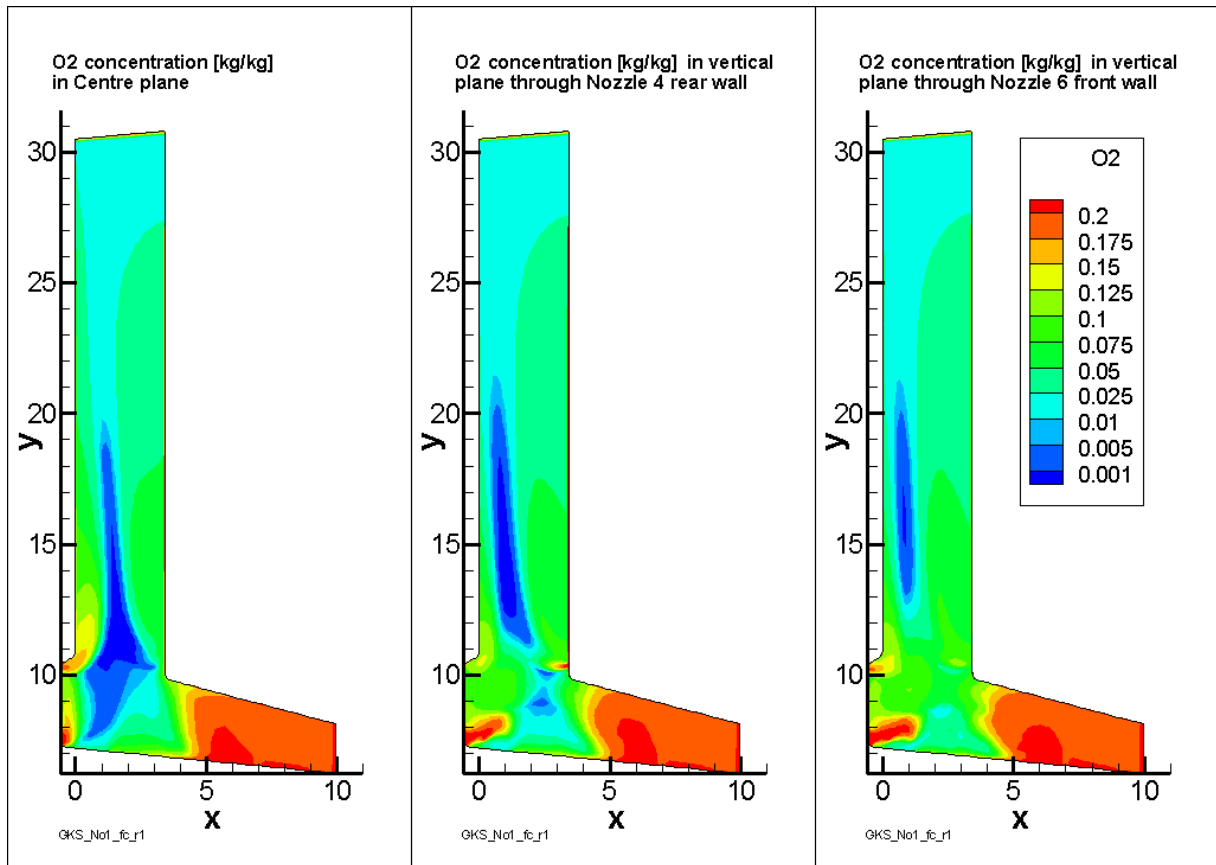


Figure 3.19 Oxygen concentration (kg/kg) shown in three different vertical planes

3.2.4 Work by GKS

3.2.4.1 Numerical tool

The main framework for the CFD calculations are done with the commercial CFD-package ANSYS-CFX 11.0. ANSYS-CFX offers an interface to implement user-defined routines. By this interface it is possible to adapt the code to special requirements

3.2.4.2 Physical models

For turbulence a modified *k- ω -model*, called *SST in ANSYS-CFX* is used.

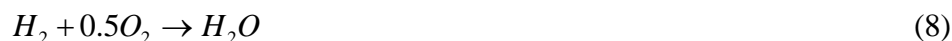
The reaction-treatment was done in 2 ways.

First is the fast chemistry approach with the Eddy Dissipation Model (EDM). This model is colloquial called “mixed is burned”. So the reaction is determined by the turbulent mixing. The EDM is suitable for fast reactions. But it is commonly known, that the reaction of CO is quite slow. To see these slow reactions, an implementation of reaction-mechanism is necessary. Total mechanism has around 50 species and a few hundred reaction-steps. The calculation for that numerical system is quite time-consuming.

To have a better ratio for quality and calculation-time we have implemented a combination of fast and detailed chemistry. All except the CO-reaction are done with the EDM. For the reaction of CO a mechanism with 17 species and 32 reactions is implemented in the EDC.

The organic components are summarized to C₃H₈.

For the EDM following reactions are considered:



For the EDC approach, reaction ($CO + 0.5O_2 \rightarrow CO_2$ (7)) is replaced by the CO-mechanism of Yetter /22/.

H₂-O₂ Chain Reactions



H₂-O₂ Dissociation/Recombination Reactions





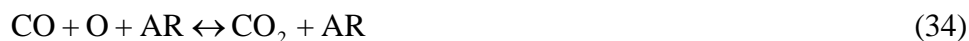
Formation and Consumption of HO₂



Formation and Consumption of H₂O₂



Oxidation of CO



Formation and Consumption of HCO



3.2.4.3 GKS-Symmetry:Geometry

The calculations are done with a symmetry model. This has the advantage of shorter calculation times but does not show imbalanced effects, which can occur with e.g. tangential inlets. For better boundary conditions a part of the second duct is incorporated. In the following figures the model is reflected by the symmetry plane.

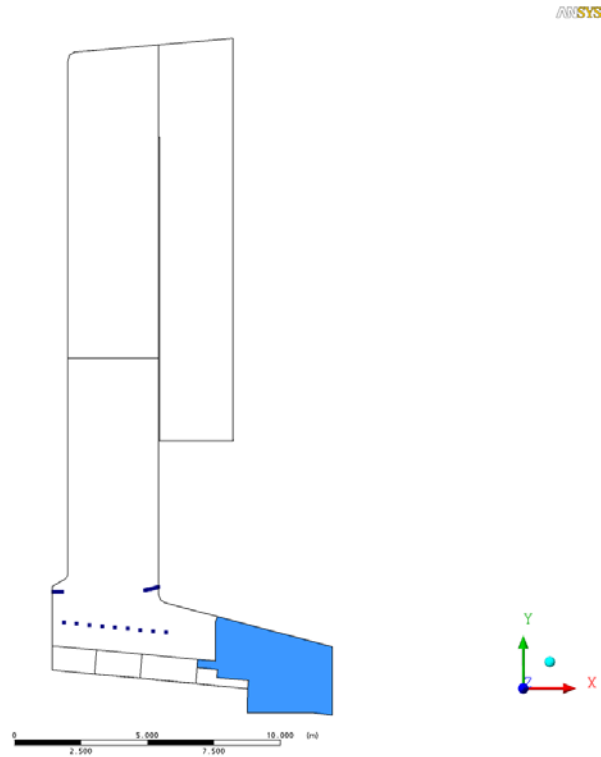


Figure 3.20 Geometry

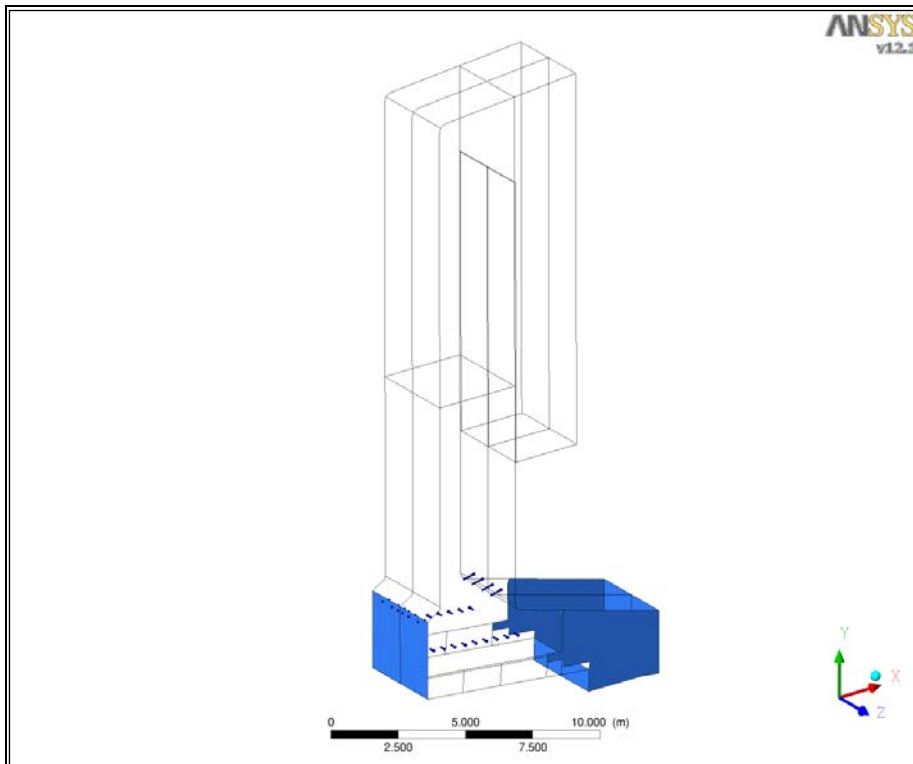


Figure 3.21 Geometry

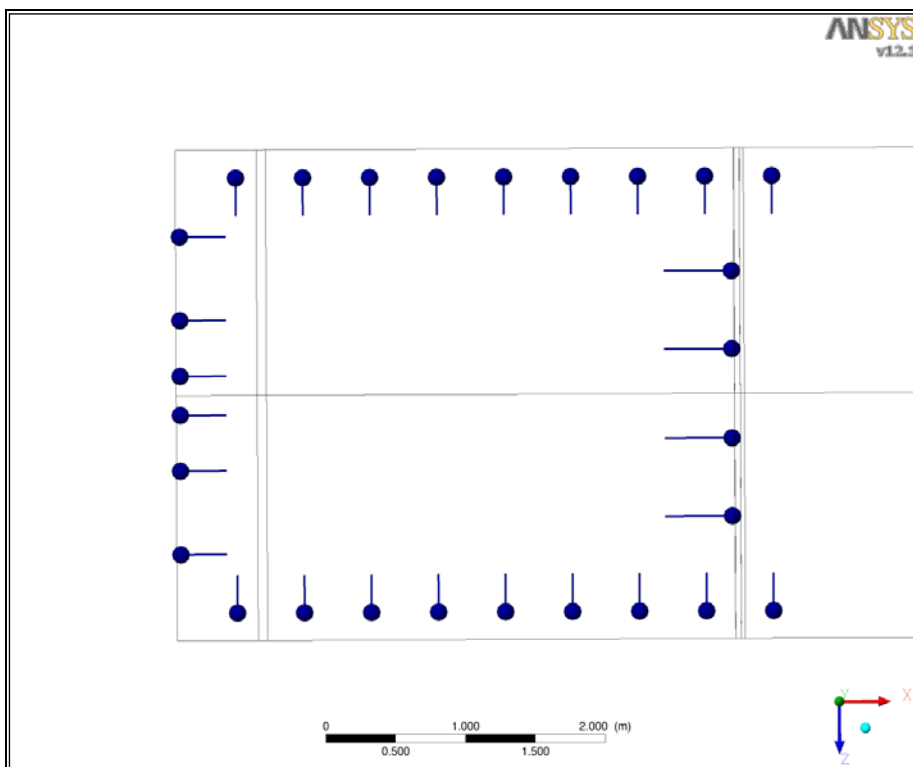


Figure 3.22 Arrangement of nozzles

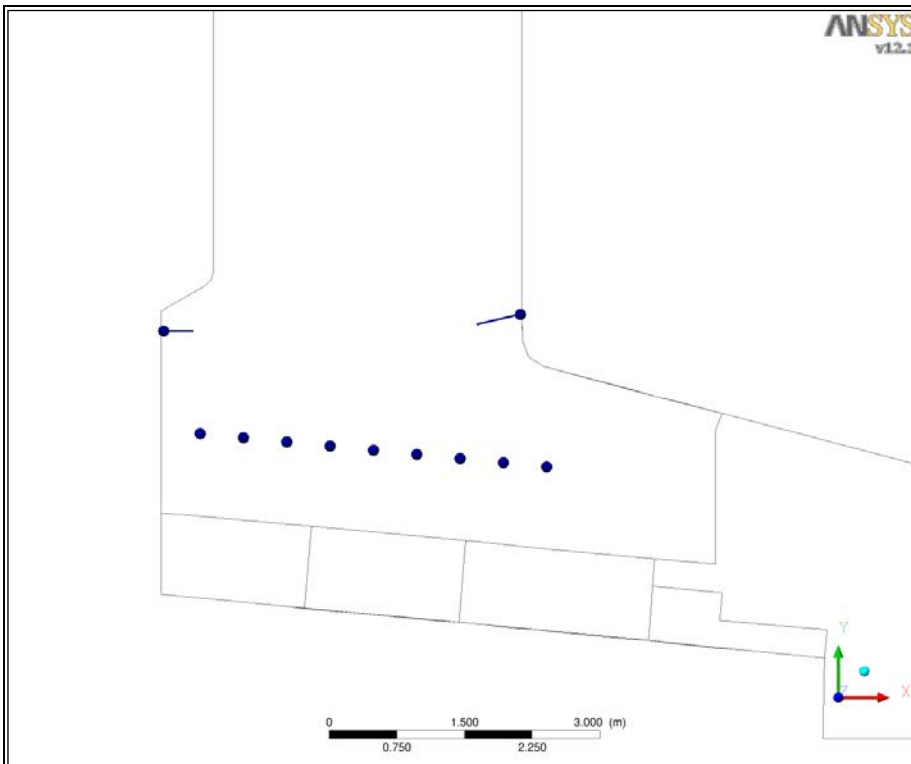


Figure 3.23 Arrangement of nozzles

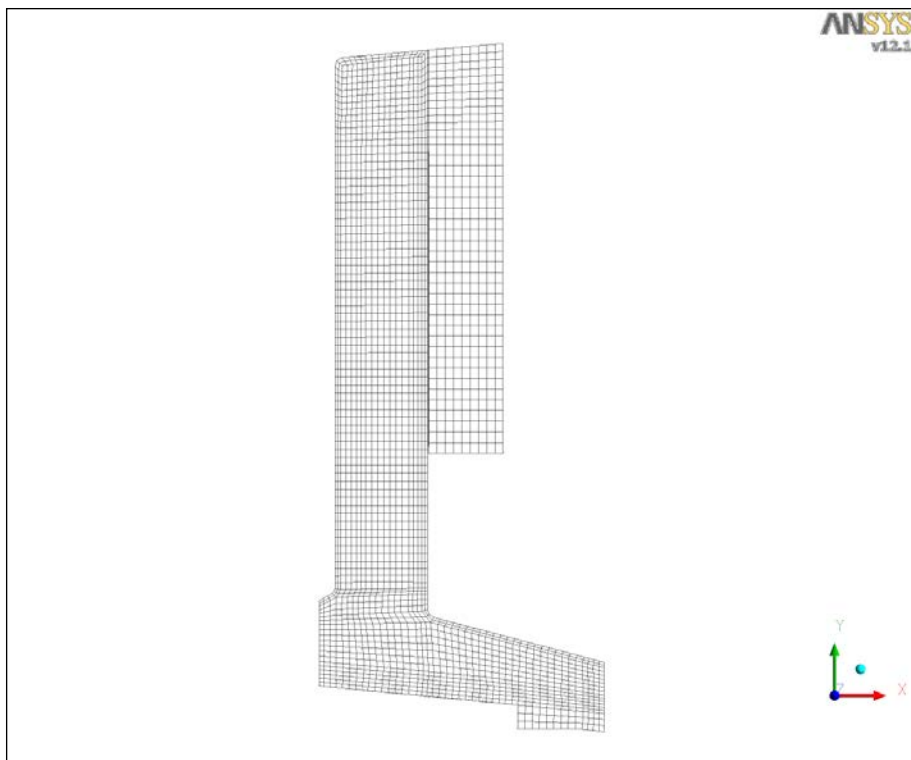


Figure 3.24 Geometry 1 / 30.000 cells

GKS-Symmetry: CFX with GKS-Model and fast kinetic

3.2.4.3.1 Temperature

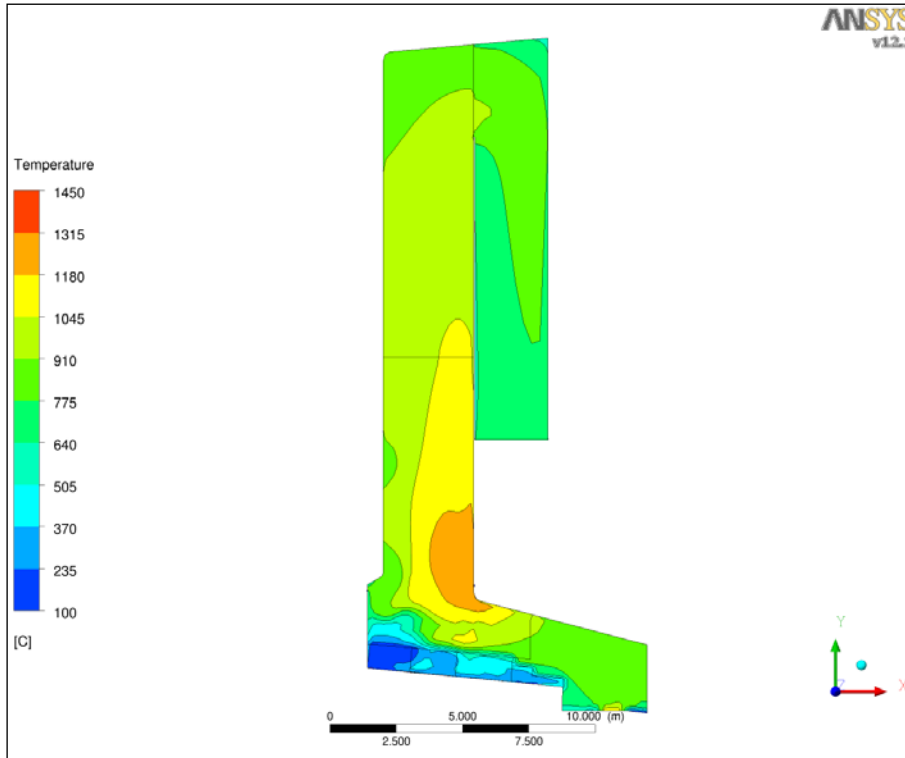


Figure 3.25 Temperature in symmetry plane

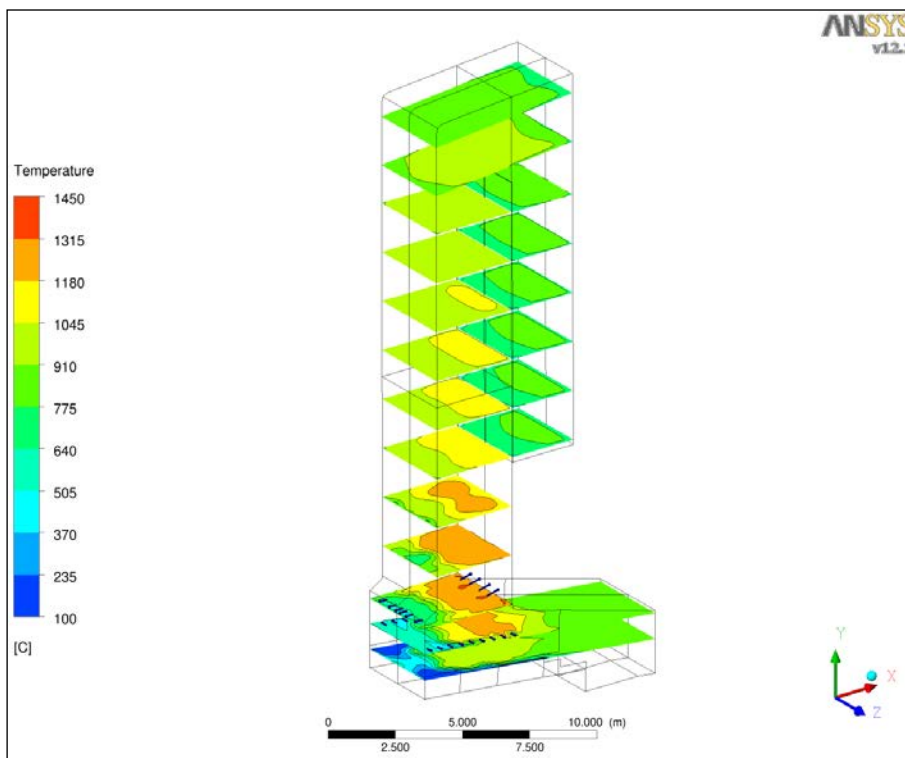


Figure 3.26 Temperature in horizontal planes

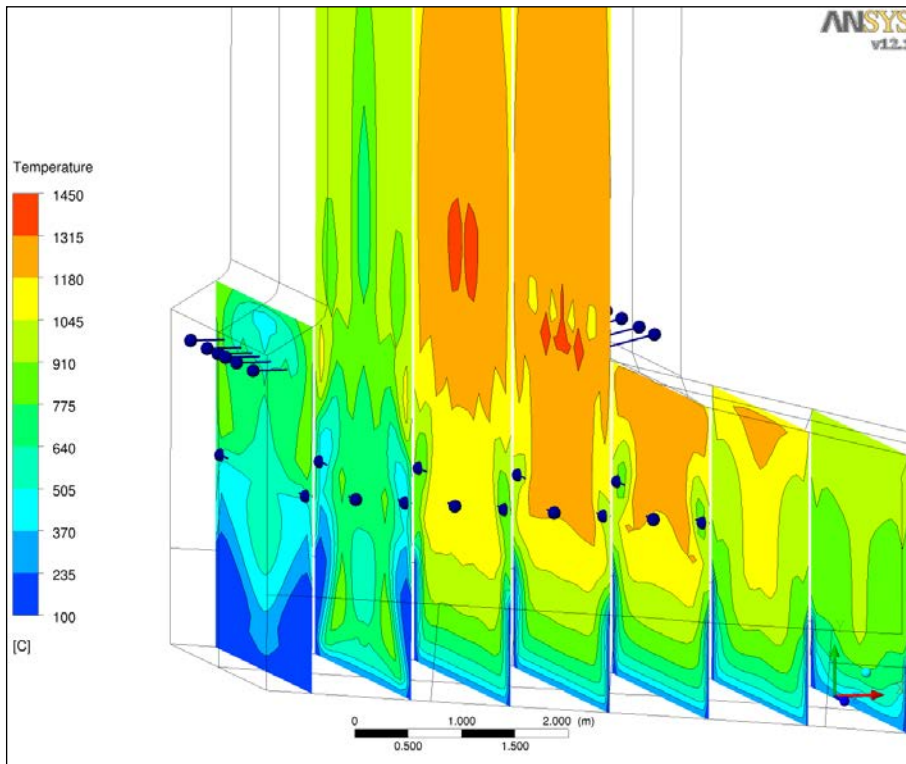


Figure 3.27 Temperature in combustion chamber

3.2.4.3.2 Velocity

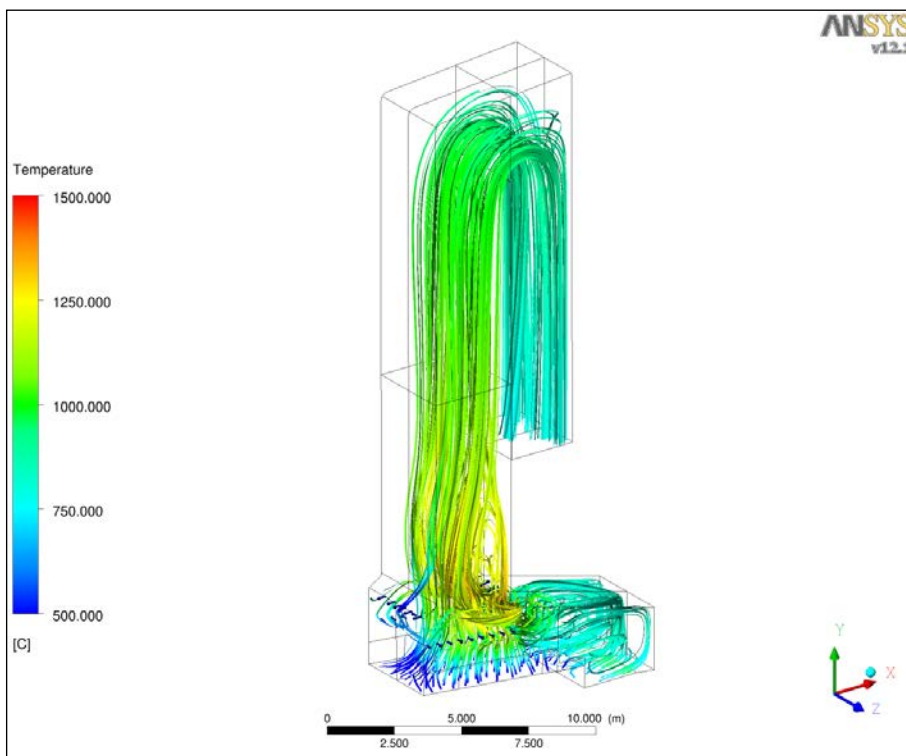


Figure 3.28 Streamlines

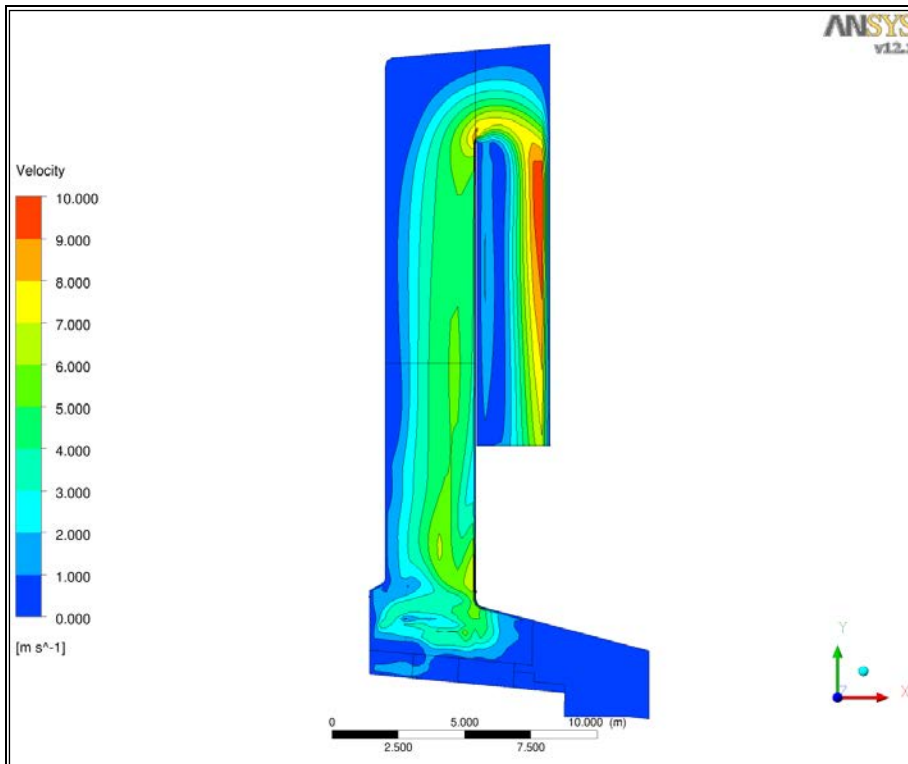


Figure 3.29 Velocity in symmetry plane

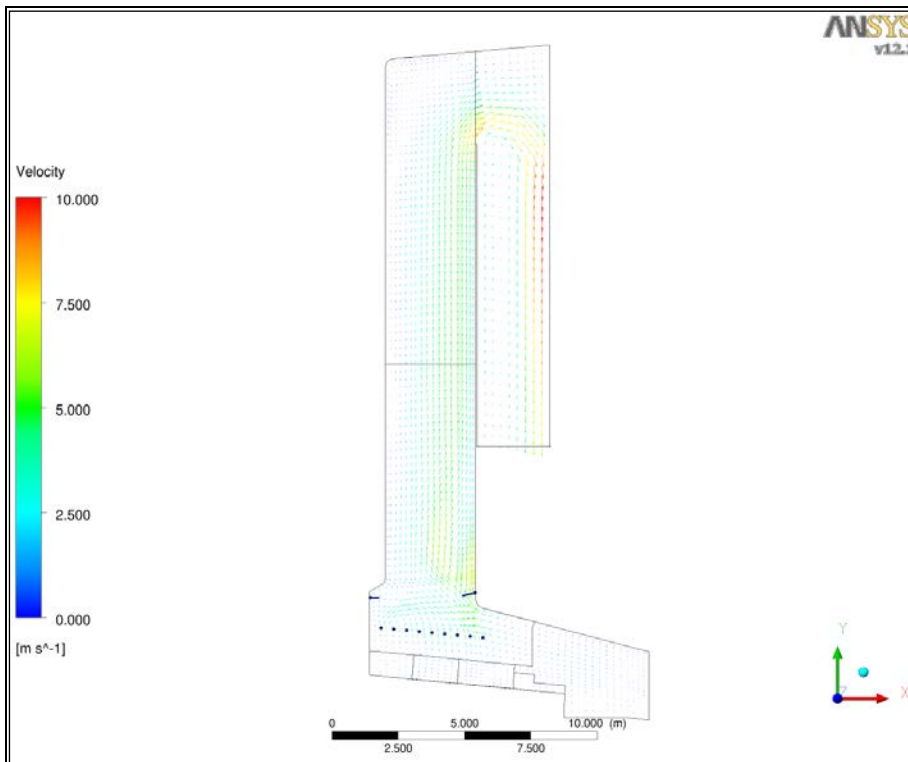


Figure 3.30 Velocity-vectors in symmetry plane

3.2.4.3.3 Species

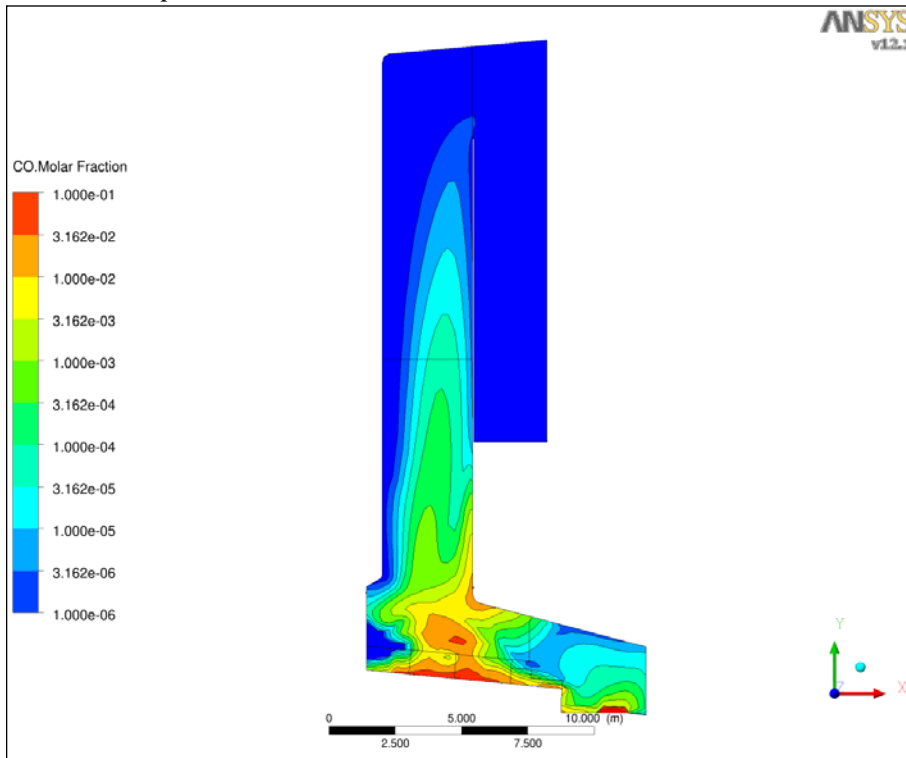


Figure 3.31 CO-distribution

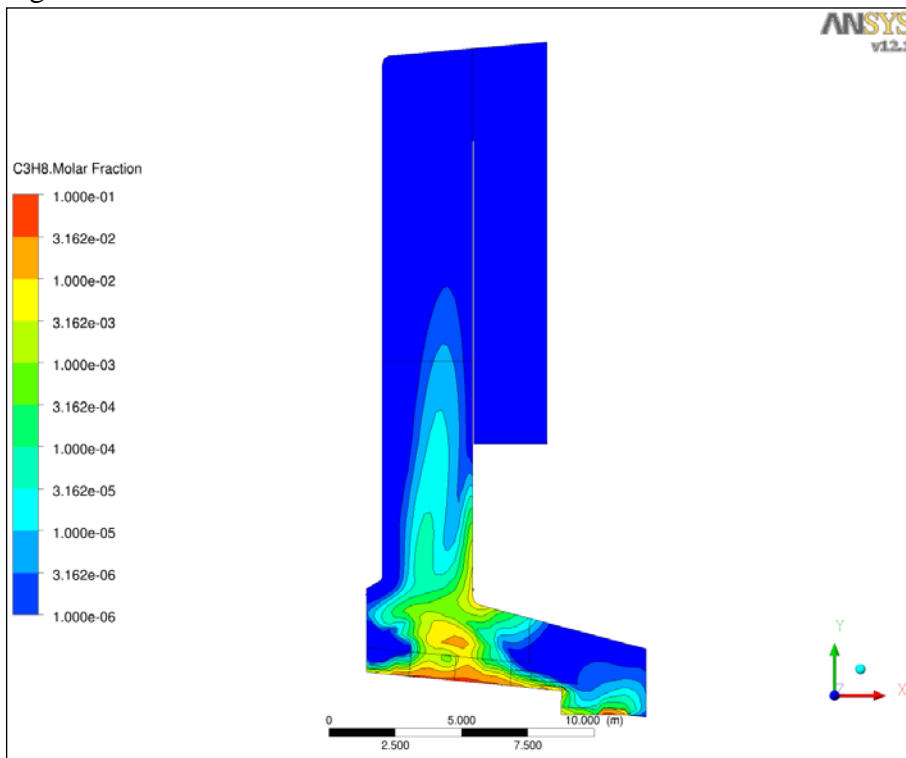


Figure 3.32 CxHy-distribution

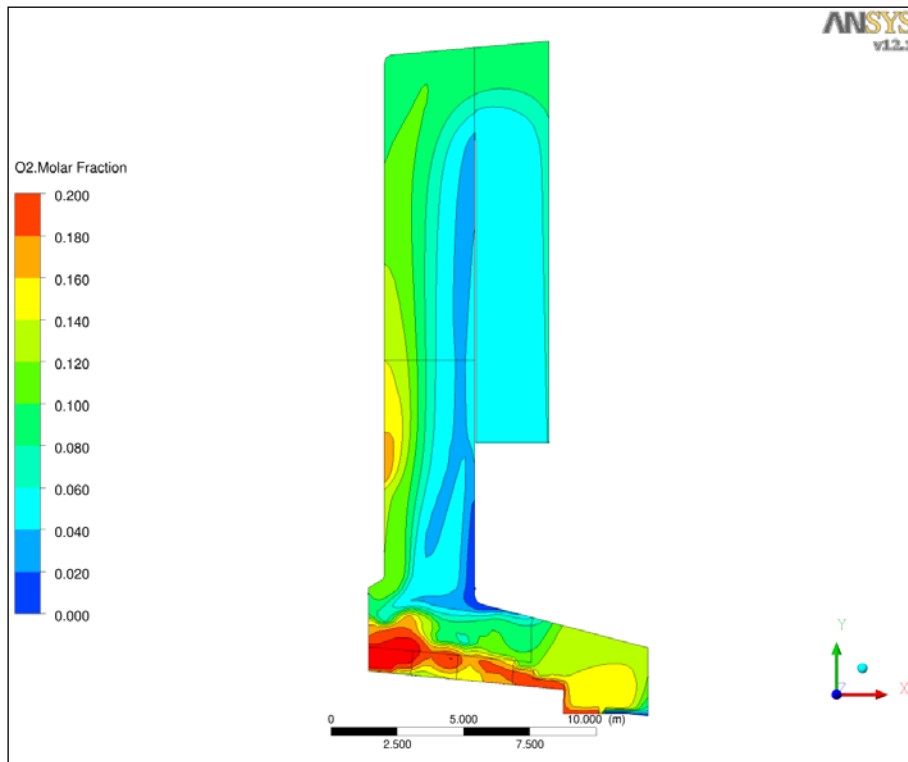


Figure 3.33 O₂-distribution

3.2.4.4 GKS-Symmetry: CFX with GKS-Model and detailed kinetic

3.2.4.4.1 Temperature

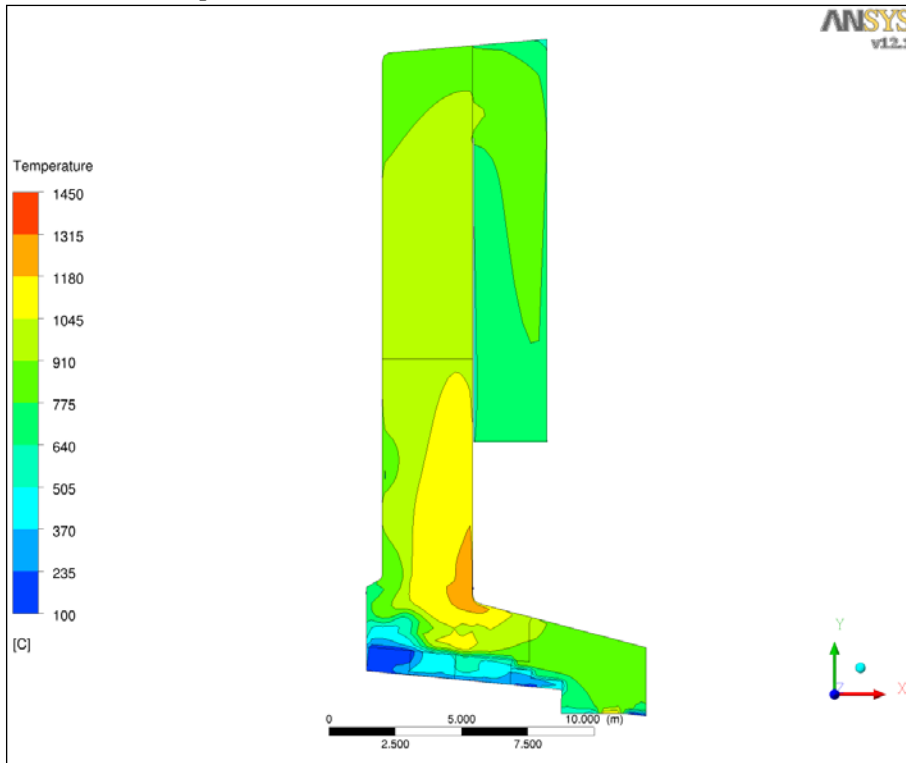


Figure 3.34 Temperature in symmetry plane

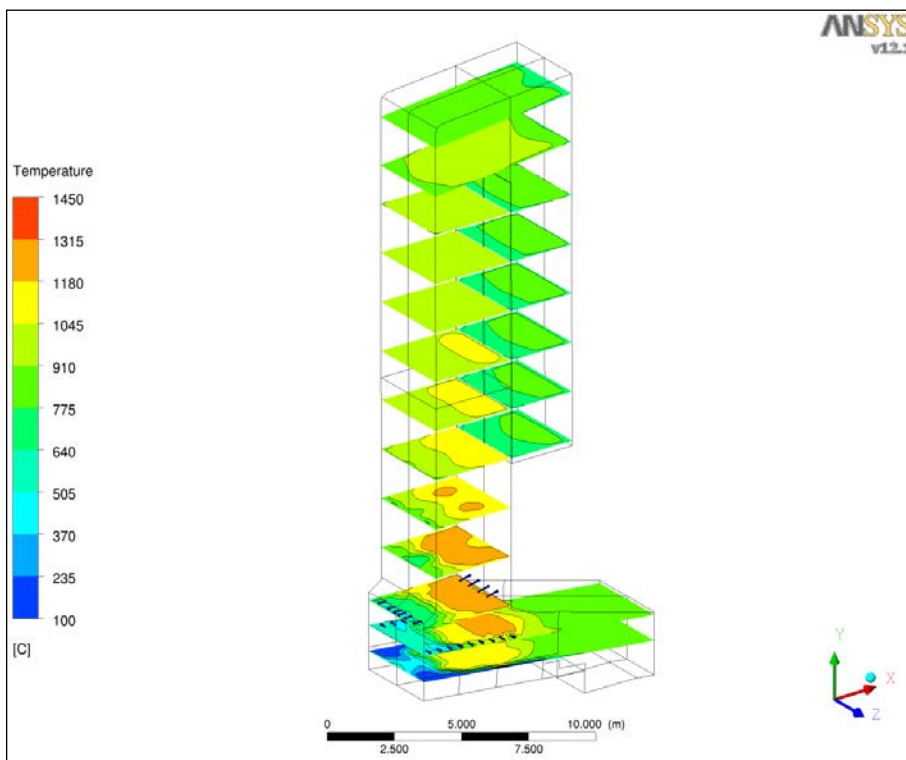


Figure 3.35 Temperature in horizontal planes

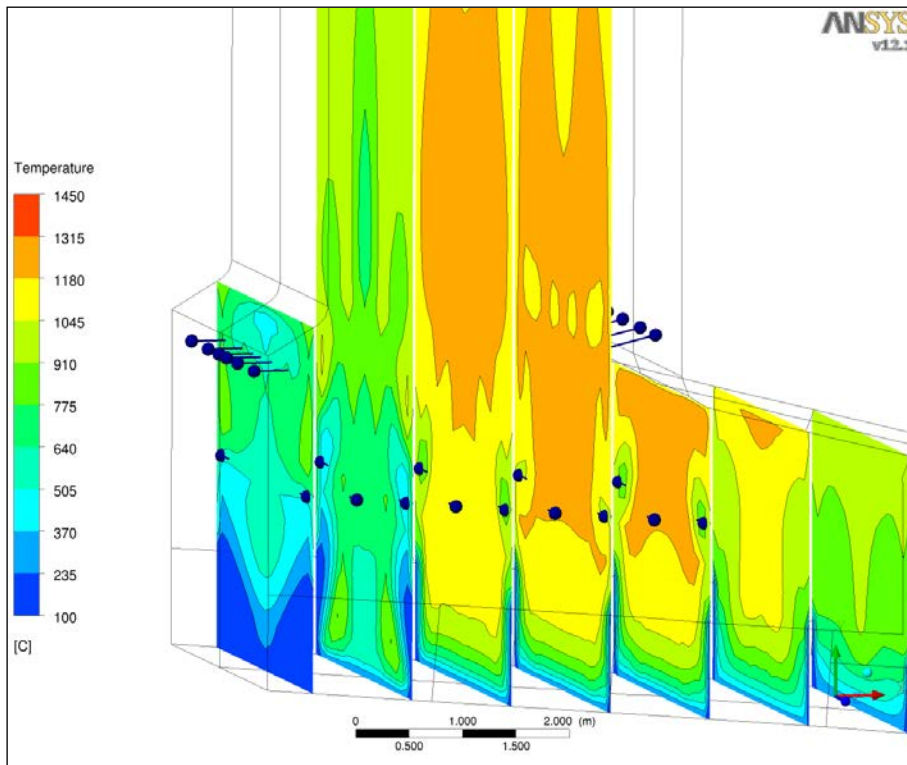


Figure 3.36 Temperature in combustion chamber

3.2.4.4.2 Velocity

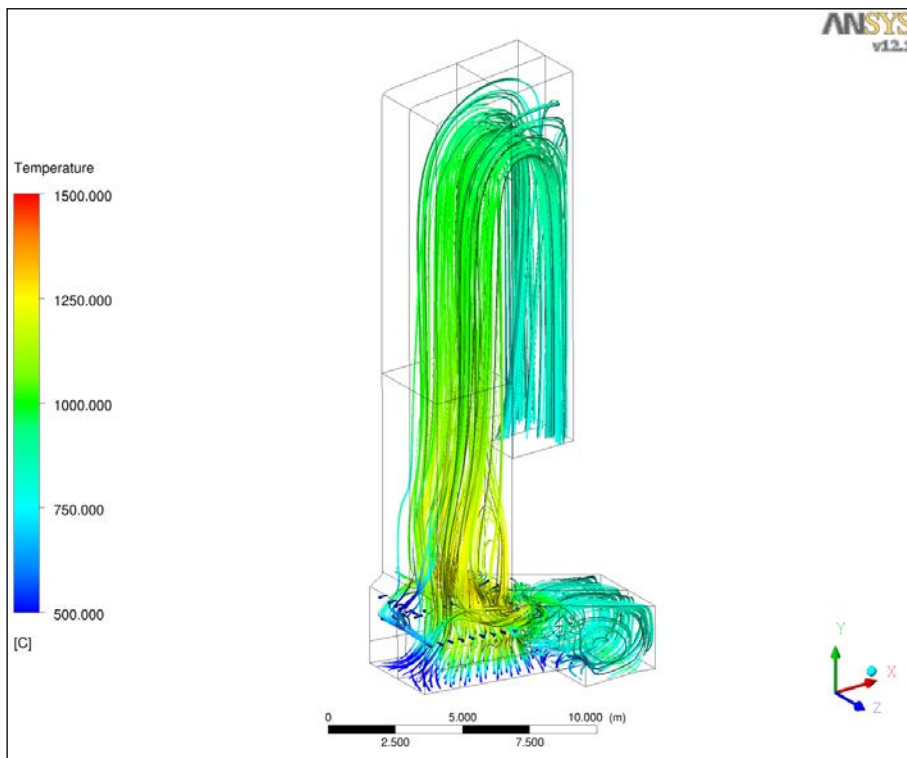


Figure 3.37 Streamlines

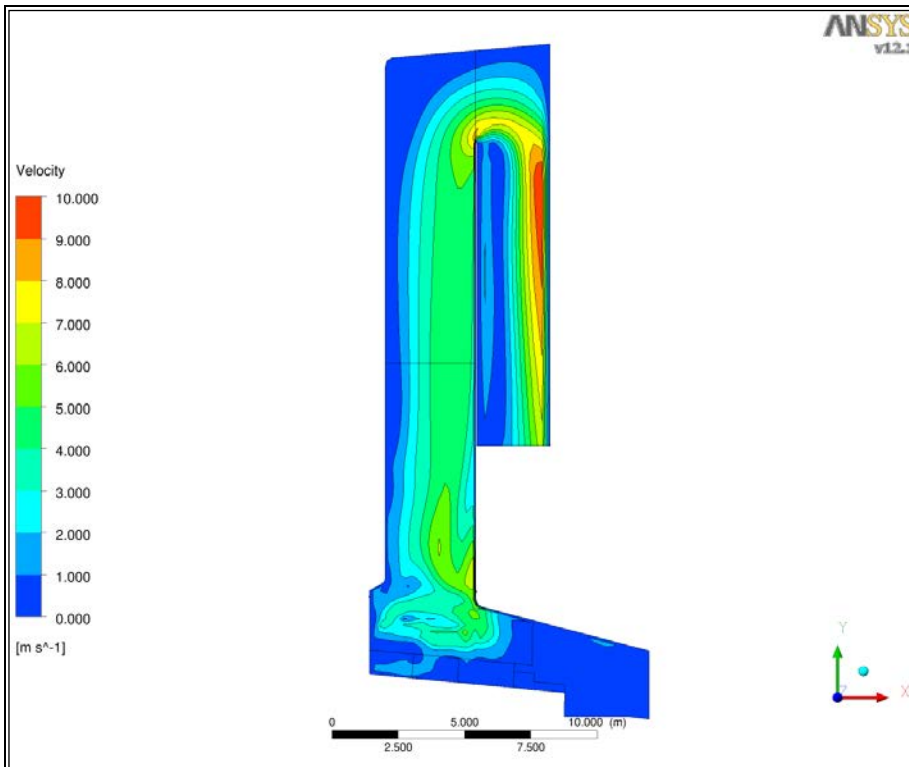


Figure 3.38 Velocity in symmetry plane

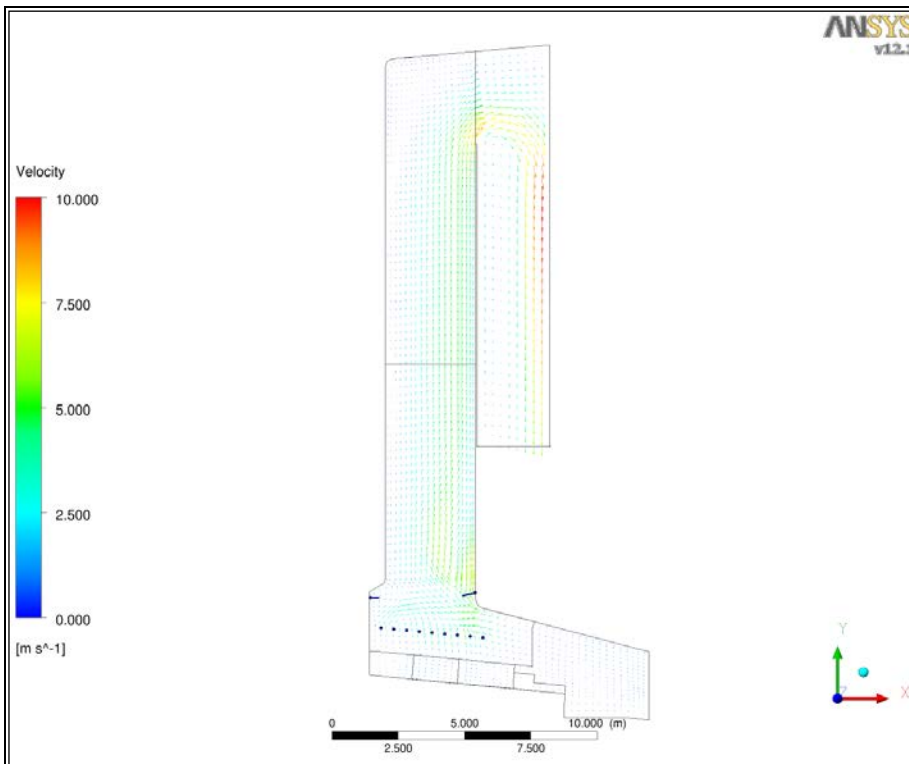


Figure 3.39 Velocity-vectors in symmetry plane

3.2.4.4.3 Species

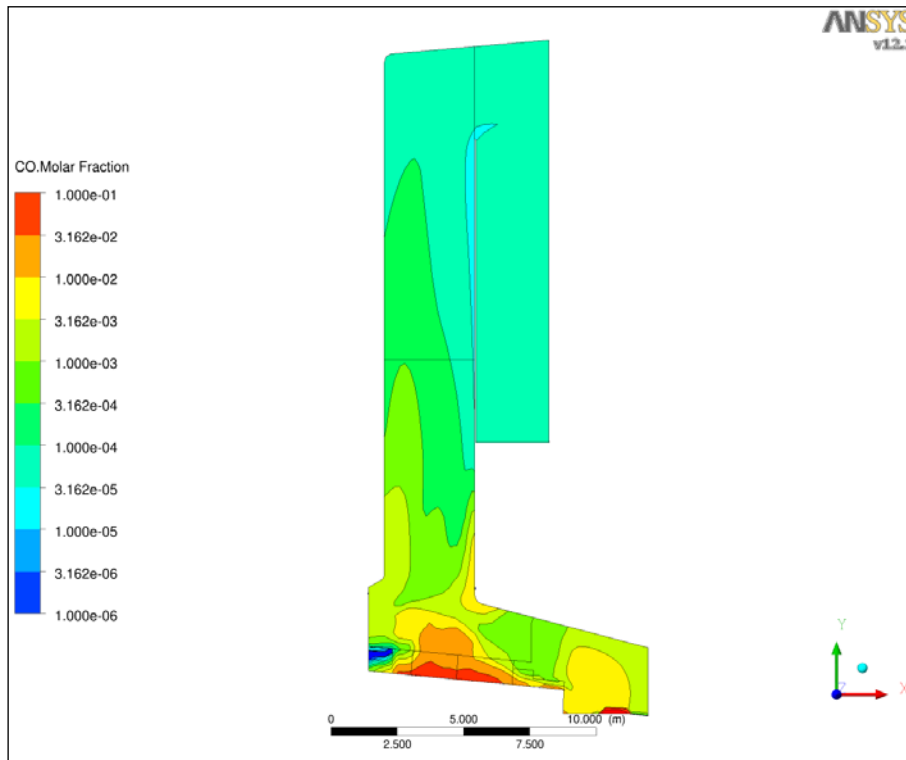


Figure 3.40 CO-distribution

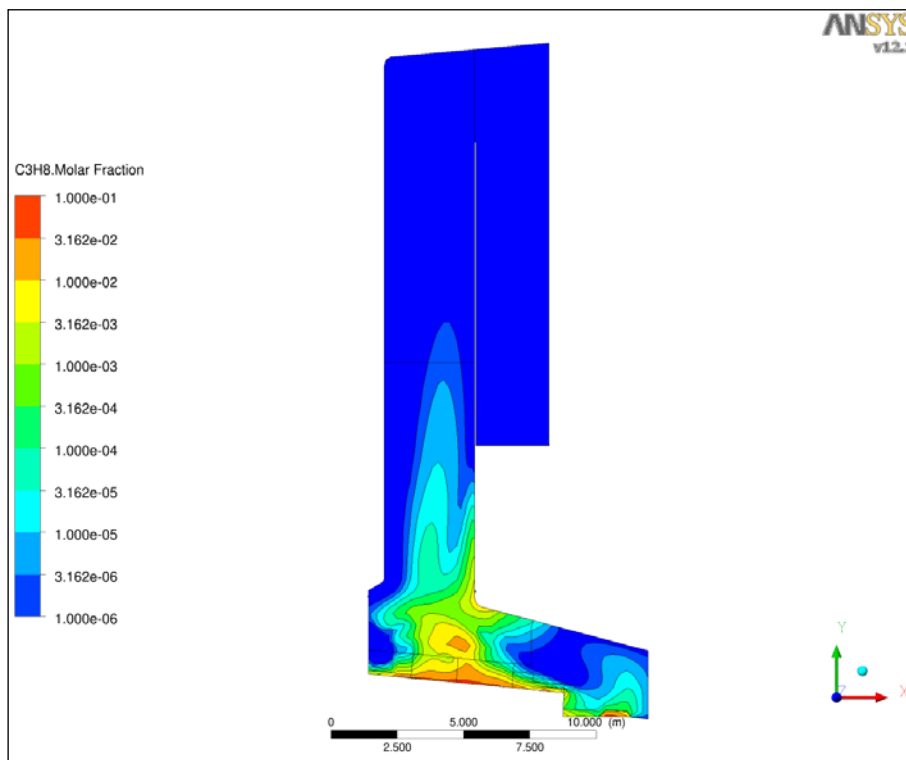


Figure 3.41 CxHy-distribution

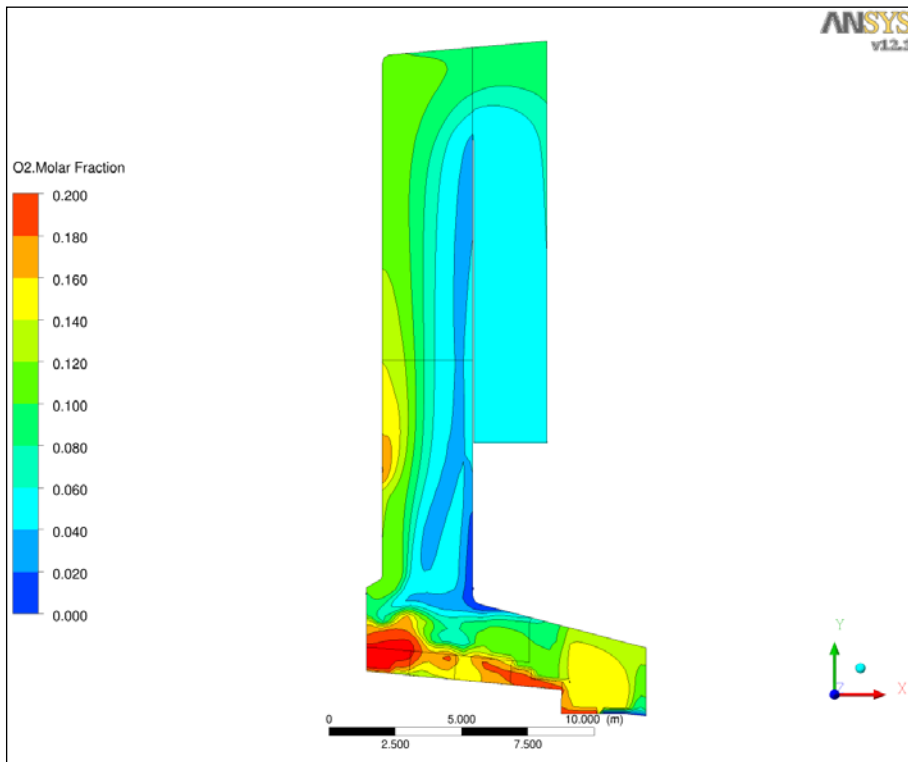


Figure 3.42 O₂-distribution

4. DISCUSSION

4.1 Differences in Simulation Tools

Principally there should not be any differences between commercial codes and in-house codes if the same models, boundary conditions and discretisation schemes are used for solvers of equal accuracy on a "grid-converged" mesh (or the very same mesh).

The advantage of an in-house code is the much greater flexibility, as all models within the code is open to the user. Some models/features that exist in in-house codes are not readily available in commercial codes, e.g. parallelized detailed chemistry.

Whereas all internals of commercial codes stays hidden to the user.

The great advantage of commercial codes are

- the ease of use,
- the robustness and
- intensive testing by a huge number of users.

4.2 Influence of CFD-code

To constitute the isolated influence of different CFD-codes is problematic, as the combination of a clutch of individual constituents form the final result of a simulation. In this comparison the maximal possible amount of similar submodels were chosen.

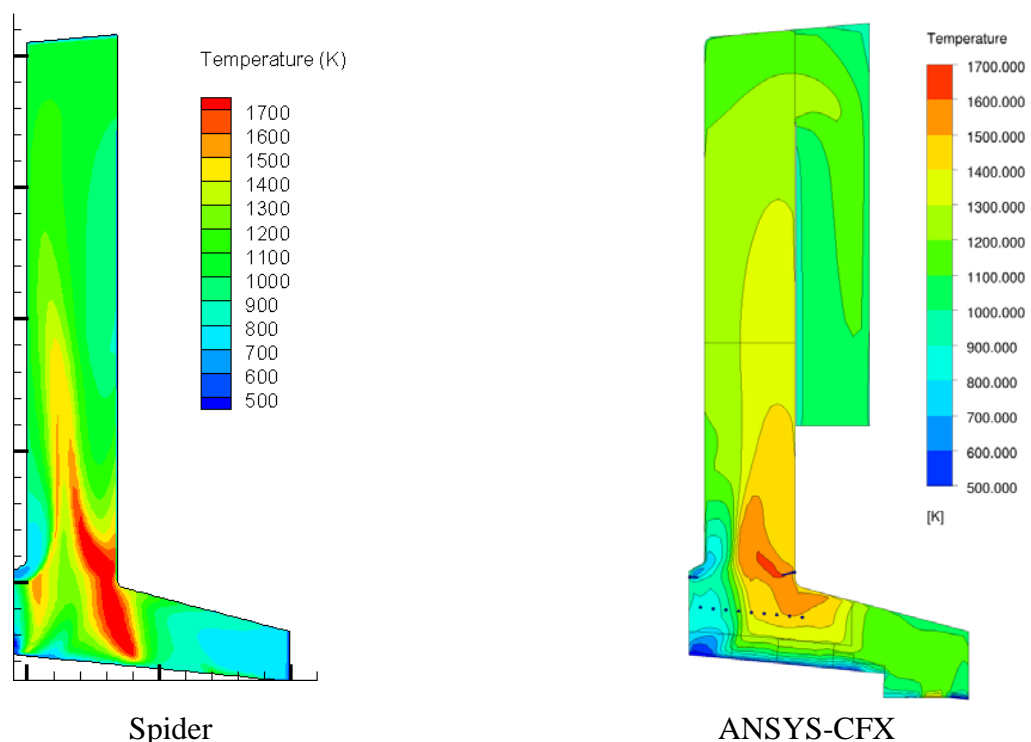


Figure 4.1 Comparison of Temperatures in Kelvin with different CFD-codes with fast kinetics

Looking at Figure 4.1 the temperature distribution resulting with different CFD-codes is quite different. Especially at the grate inlet the CFX-calculation shows a lower temperature, which obviously is caused by the radiation to the bed. Another remarkable discrepancy is the region of waste feed. The drying region normally show lower temperature even when first combustion will occur within that region.

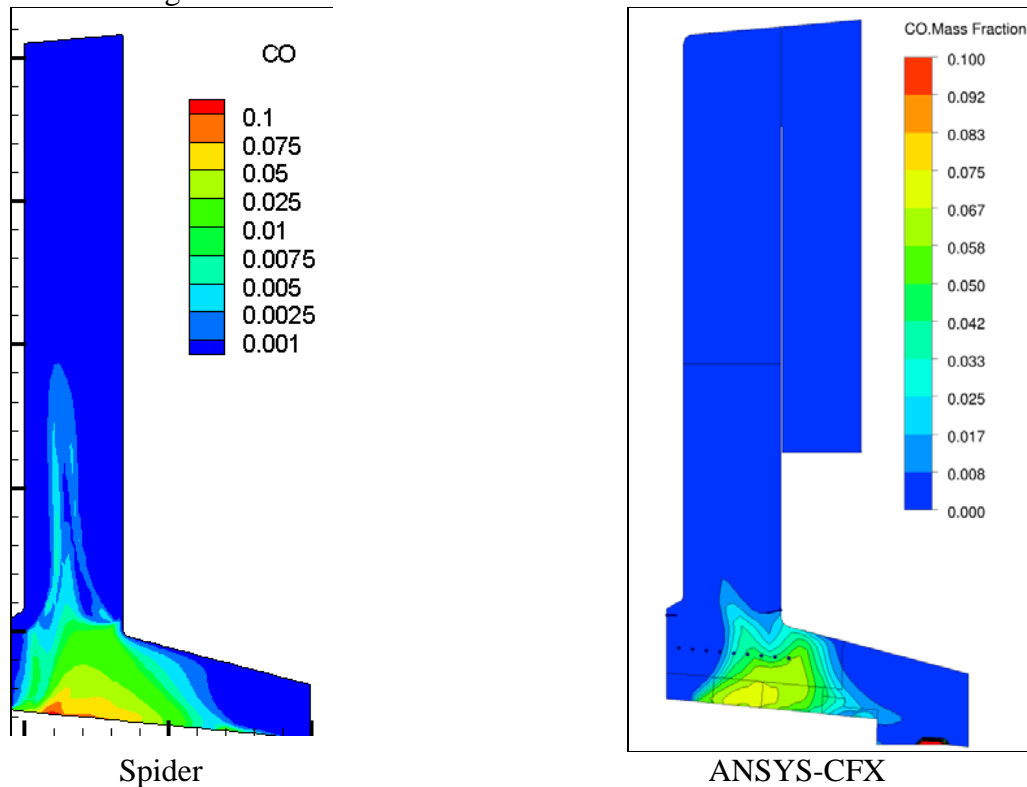


Figure 4.2 Comparison of CO-distribution with different CFD-codes with fast kinetics

The region of remarkable CO-fractions is greater in the spider calculation. This could be grounded by the more sophisticated chemistry model at spider. But remembering Figure 4.1, the higher temperatures leads to higher velocities and therefore shorter reaction-times in a specified region. More precise information could be done with a complete detailed chemistry approach, which was aspired by Sintef. By numerical problems no evaluable results from Sintef are on hand by now.

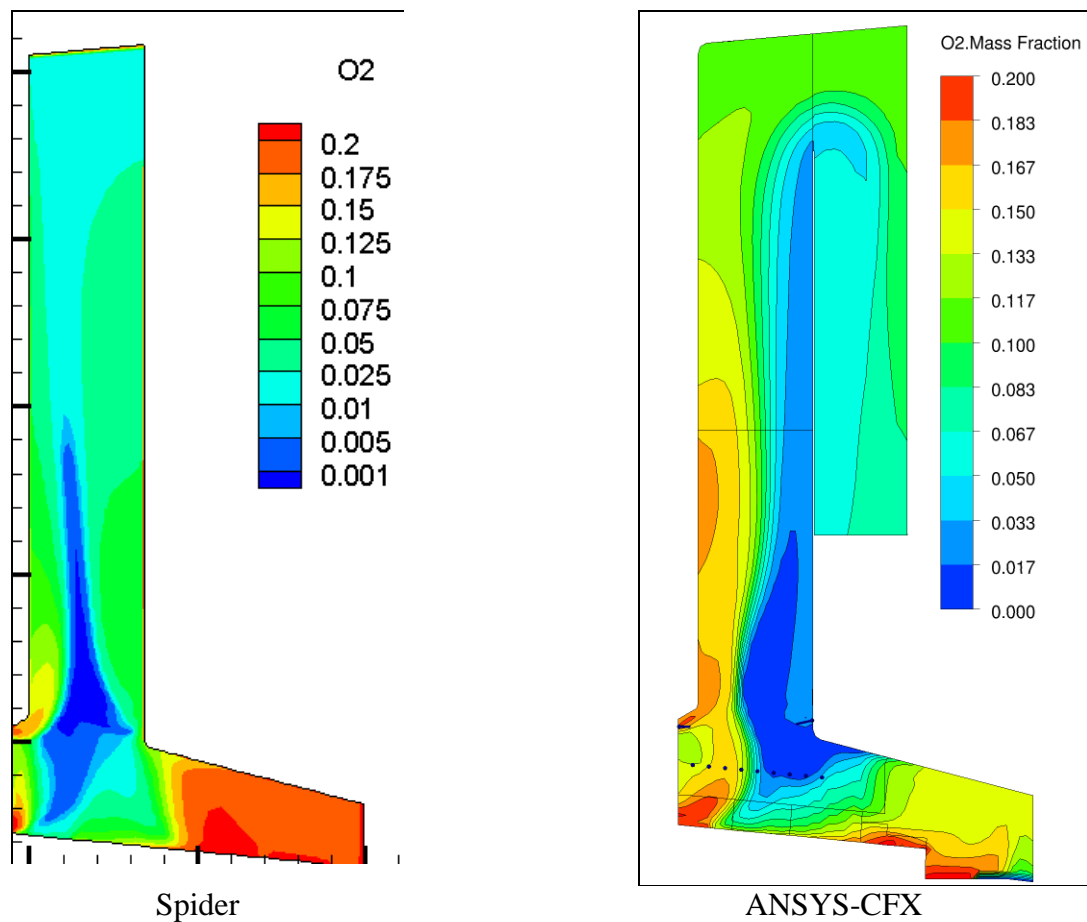
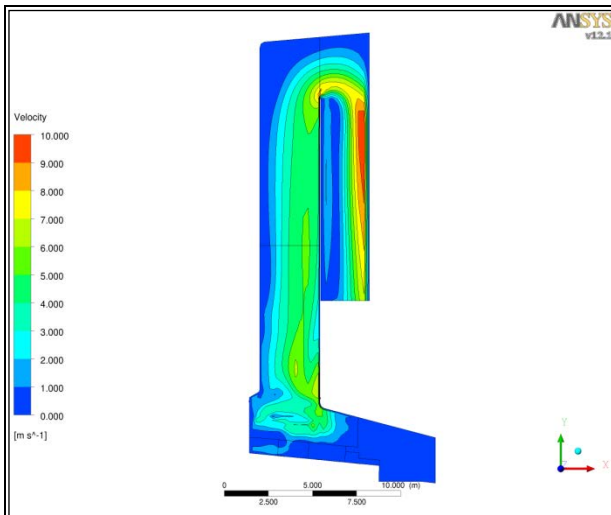


Figure 4.3 Comparison of O₂-distribution with different CFD-codes with fast kinetics

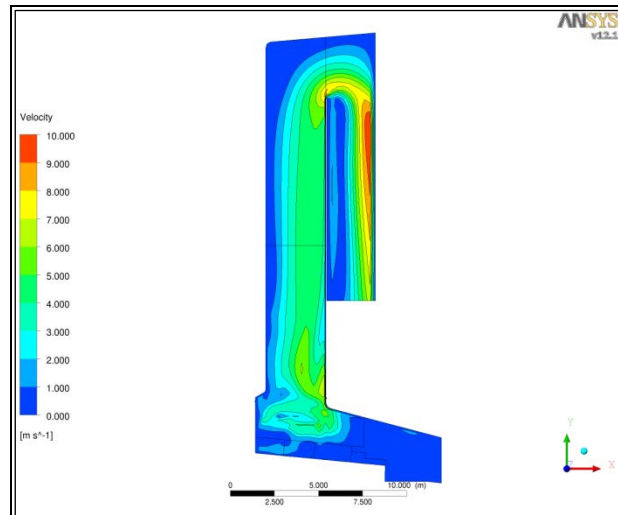
The biggest difference is detected for the O₂-distribution. At the CFX-simulation very low O₂-fractions are found at the rear wall of the 1st duct. The reason for that cannot be clearly stated, as the combination of discrepancies described above and some more differences could multiply to those results.

4.3 Influence of chemistry concept

Global reaction-schemes neglect the influence of by-products. For the global sight to the simulation, which will offer e.g. velocities or temperature-distribution, a global scheme is satisfactory.



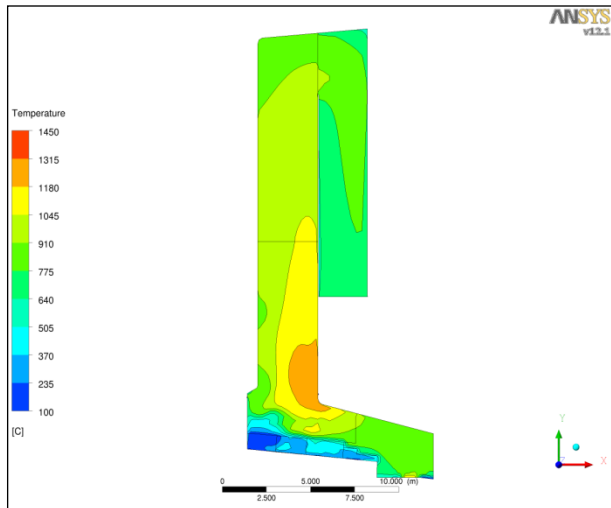
Fast chemistry



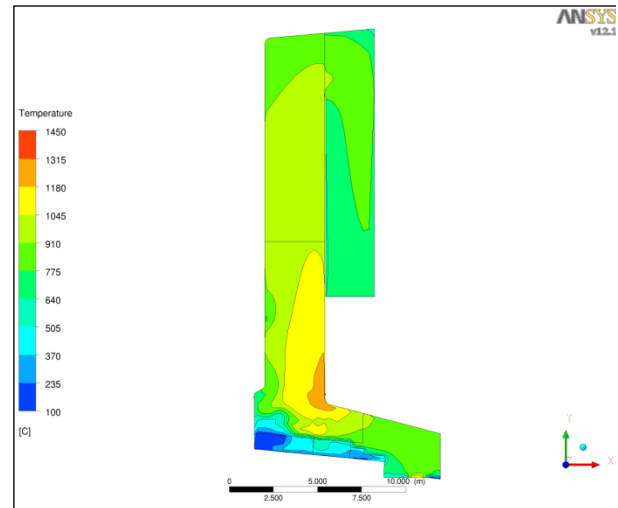
Detailed chemistry

Figure 4.4 Comparison of velocities with different reaction schemes

In Figure 4.4 is shown that the velocity field with fast-chemistry and detailed chemistry is quite similar.



Fast chemistry



Detailed chemistry

Figure 4.5 Comparison of temperature with different reaction schemes

Beside local differences in temperature the overall distribution is rather independent to the chemistry-approach (see Figure 4.5).

But if detailed information is necessary for some species, there is no way but implementing detailed mechanisms that will meet the demands.

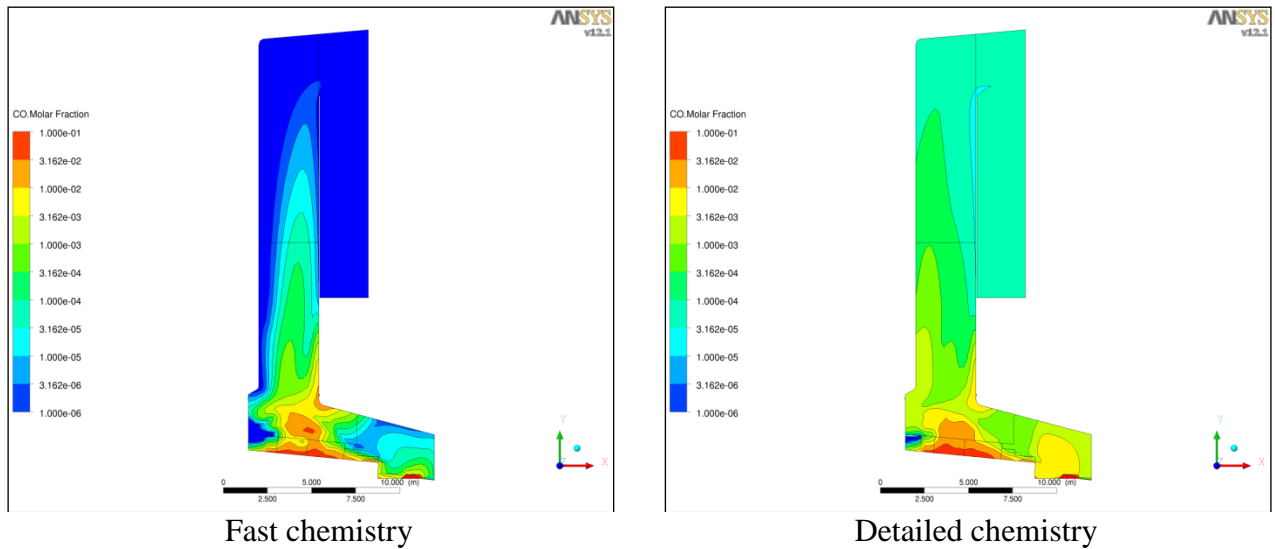


Figure 4.6 Comparison of CO with different reaction schemes (logarithmic scale)

Depending of the chemistry sub model for CO-consumption a big difference can be seen. The implemented detailed chemistry sub model includes reactions steps with H_2O and derived radicals. So a strong influence for e.g. added steam should be noticeable. On the other hand the number of cells is quite low (about 30.000). Looking to D2.6.12-Part 2, where had been made a simulation with about 2 Mio. cells and fast chemistry (see there Fig. 6.1.1), the CO distribution is close to that of Sintef and the version with detailed chemistry. It can be stated that the low number of cells has a more negative impact on the simulation results concerning the flow than the kind of chemistry.

4.4 Influence of concept of bed model

The fuel bed model (FBM) is a separate tool to get meaningful boundary conditions for the outlet from the fuel bed, which is an inlet for the CFD calculation. The 2 bed models which had been compared can be seen in D2.6.25.

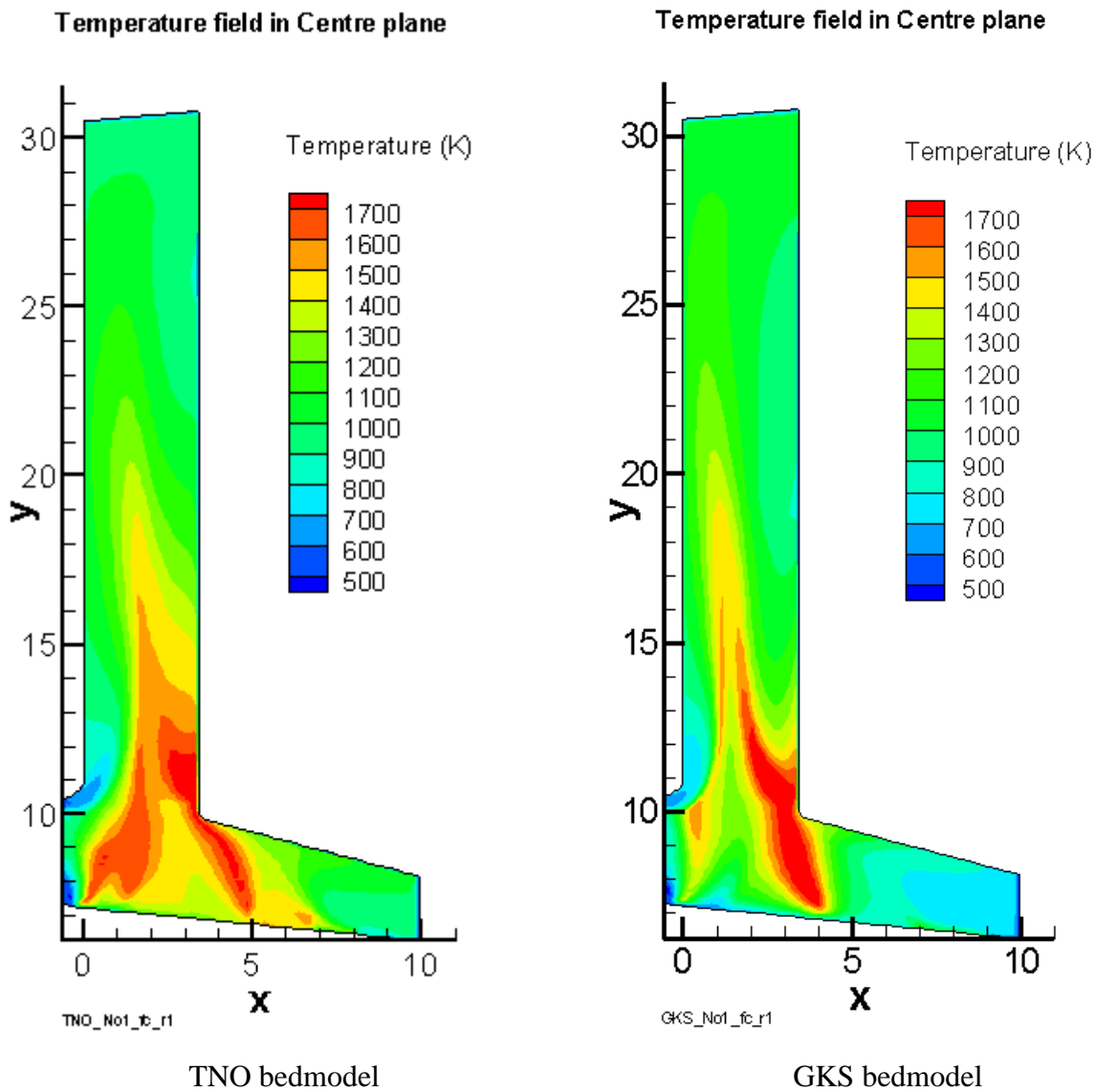


Figure 4.7 Comparison of temperature with different bedmodel and Spider

As a first view (Figure 4.7) the temperature distribution is similar. In the front of the combustion chamber (left side) there is a greater region of higher temperature. Even at the beginning of the first duct the regions of higher temperature reach further up.

The reason seems to be an earlier start of the degassing process from the solid fuel in the TNO-FBM (see Figure 3.4 and Figure 3.5). This can be also seen in Figure 4.8 and Figure 4.9.

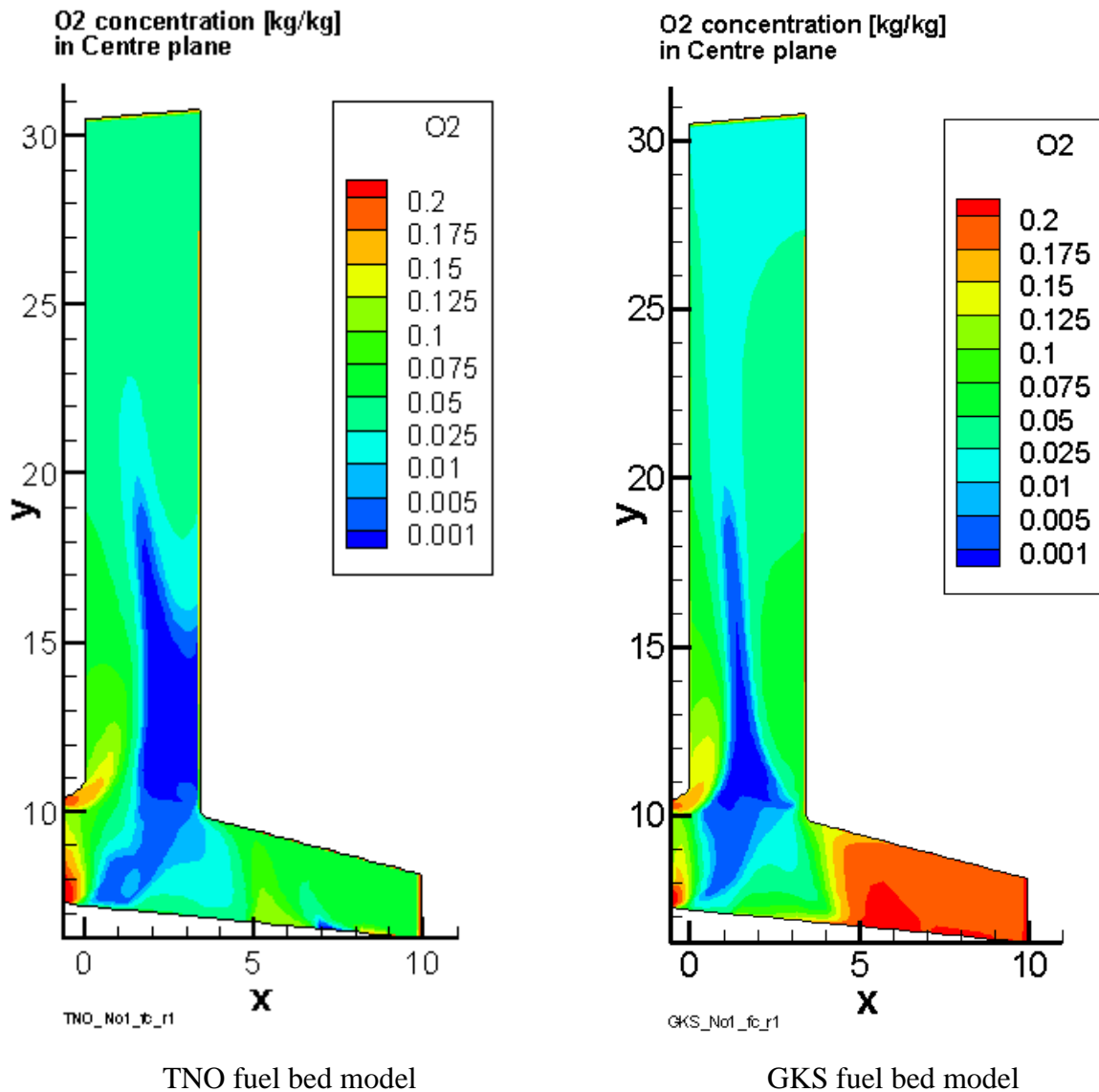


Figure 4.8 Comparison of O₂-distribution with different fuel bed models and Spider-code

The primary air distributions in both simulations are identical. For that the greater region of low O₂ at the first ¼ of the combustion chamber indicates a higher consumption of O₂ and for that a higher level of combustibles. The low content of O₂ in the TNO-FBM is not realistic because measurements (see D2.6.12-Part 1) have shown, that the O₂ content at the end of the grate is quite high. The low content of the TNO-FBM at the end of the grate can be a result of a higher coke content in the bed there.

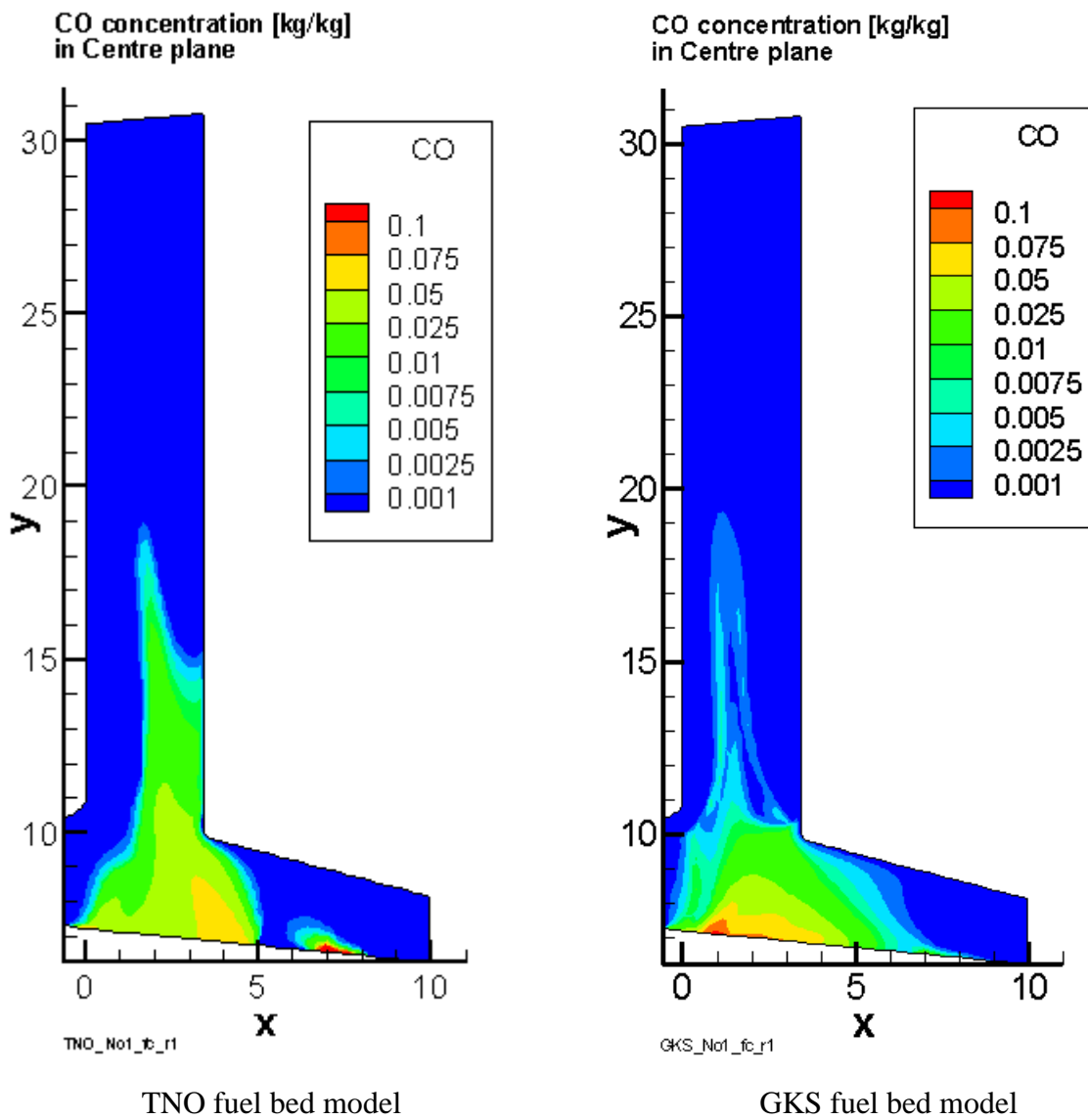


Figure 4.9 Comparison of CO-distribution with different bed model

The distribution of CO in Figure 4.9 shows a distinguished gap along the grate at around 5.5m. At about 7 m there is a very low mass flow for primary air, which seems to generate more CO with the TNO-FBM (see Figure 3.4 and Figure 3.5).

5. SUMMARY AND OUTLOOK

It can be stated, that the biggest influence to the results are caused by the boundary conditions. Waste incinerators handle a very complex solid fuel, which cannot be described with a small set of empirical equations. In fact an individual simulation tool is needed to describe the effects in the waste-layer. But unlike CFD-simulation tools, which always try to solve a given set of equations (Navier-Stokes) the processes in the fuel-bed are not defined scientifically. By that, individual bed-models must have different results, as the individual submodels are based on subjective observations.

The number of discrete cells has an impact to the results which seem to be much bigger than the chose of the CFD model. Measurements in the plant show that a higher CO content lays at the front wall. While 30.000 cells with a fast chemistry seem to be too less because the CO content is higher at the rear walls side, 70.000 deliver better results. Use of detailed chemistry brings better results even with less cells. Best results for CO distribution can be delivered with a high amount of cells (about 2 Mio.) and detailed CO-chemistry (see D.2.6.12-Part2).

The fuel bed model gives a very strong impact to the results. There could have been detected very strong differenced in the burnout zone of the grate.

The combustion process is normally handled by the fast-chemistry approach, which is warrantable for most cases (when the number of cells is adequate). If there is specific interest to the chemical process, dedicated sub-models must be implemented. Unfortunately the Sintef detailed chemistry model had not been ready for this deliverable to be compared to the GKS detailed chemistry model.

As a rule of thumb it can be stated, that it must be contemplated, what the goal of a simulation should be, as the adding of sub-models will not increase the computational effort by factors but by dimensions.

Nevertheless the simulations give a good indication what the processes in the combustion are when general rules had been considered and an adequate boundary conditions for the fuel bed model can be choosen.

Further investigations on fuel bed model and chemistry has to be undertaken to get reliable results. For that a cooperation of Sintef and GKS would be promising.

6. LITERATURE

1. Melaaen, M.C., "Analysis of curvilinear non-orthogonal coordinates for numerical calculation of fluid flow in complex geometries", Ph.D. thesis, The Norwegian Institute of Technology, 1990
2. Gran, I.R., "Mathematical modeling and numerical simulation of chemical kinetics in turbulent combustion", Ph.D. thesis, The Norwegian Institute of Technology, 1994
3. Magnussen, B.F., "The Eddy Dissipation Concept, A Bridge Between Science and Technology", ECCOMAS Thematic Conference on Computational Combustion, Lisbon, Portugal, 21-24 June, 2005
4. Gran, I.R. and B.F. Magnussen, "A numerical study of a bluff-body stabilized diffusion flame. Part 2. Influence of combustion modeling and finite-rate chemistry", *Combustion Science and Technology*, 119, pp. 191-217, 1996
5. Kee R. J., Rupley F. M. and Miller, J. A. CHEMKIN-II, A Fortran chemical kinetics package for the analysis of gas-phase chemical kinetics. Technical report, SAND89-8009, Sandia National Laboratories, Livermore, CA, 1989
6. Melheim, J.A., "Spider: Conversion to Chemkin", Restricted Report, SINTEF Energy Research, 1999
7. Smith, G. P., Golden, D.M., Frenklach, M., Moriarty, N. W., Eiteneer, B., Goldenberg, M., Bowman, C.T, Hanson, R. K., Song, S., Gardiner Jr., W. C., Lissianski, V. V., Qin, Z., Gri-Mech 3.0, http://www.me.berkeley.edu/gri_mech/ 1999
8. Weydahl, T Bugge, M, Gran, I.R. and Ertesvåg, I.S "Computational Modeling of Nitric Oxide Formation in Biomass Combustion" *Int. J. of Appl. Mechanics in Engineering*", No.1, Vol.7, pp.125-141, 2002
9. Weydahl, T., Inge R. Gran and Ivar S. Ertesvåg, "Prediction of nitric oxide formation in ammonia-doped turbulent syngas jet flames", 1st Biennial Meeting, The Combustion Institute, 2001
10. Gruber, A and Luckerath, R "Numerical and Experimental Investigation of High Pressure Gas Turbine Model Combustor Fuelled with Hydrogen", Paper in preparation
11. Kleiveland, R.N., I.R. Gran and B.F. Magnussen, "Modeling of Soot Formation and Oxidation in Turbulent Diffusion Flames", 1st Biennial Meeting, The Combustion Institute, 2001
12. Bakken, J., A. Gruber, M. Seljeskog and T. Weydahl, "Verification of Spider", Report, SINTEF Energy Research, 2001
13. Ertesvåg, Ivar S., Bjørn F. Magnussen, 2000, "The eddy dissipation turbulence energy cascade model", *Comb. Sci. Technol.* 159: 213-236
14. Ertesvåg, Ivar S., 2000, "Turbulent strøyming og forbrenning", ("Turbulent flow and Combustion"; in Norwegian.), Tapir Academic Publisher, Trondheim
15. Glarborg P, Alzueta M.U, Dam-Johansen K, Miller J.A: "Kinetic Modeling of Hydrocarbon/Nitric Oxide Interaction in a Flow Reactor", *Combustion and Flame* 115:1-27, 1998
16. Deuflhard, P., E. Hairer and J. Zugck, 1987, "One-step and Extrapolation Methods for Differential-Algebraic Systems", *Numerische Mathematic*, 51(5), 501-516
17. R. van der Welle, "A full-scale demonstration of a stationary CFD model EU-project", NextGenBioWaste, deliverable D 2.5.9, 2008
18. A.R.J. Arendsen Modelling of biomass combustion process, EU-project OPTICOMB, deliverable 9, 10 and 12, I&T-A 2007-005

- 19.B.F. Magnussen, B.H. Hjertager “On mathematical modelling of turbulent combustion with special emphasis on soot formation and combustion”In: Proceedings of the 16th Symposium (International) on Combustion, pp. 719–229, The Combustion Institute (Ed.), Pittsburgh, USA, 1976
- 20.R. Scharler, M. Forstner, M. Braun, T. Brunner, I. Obernberger, “Advanced CFD analysis of large fixed bed biomass boilers with special focus on the convective section”, 2nd World Conference and Exhibition on Biomass for Energy, Industry and Climate Protection, 10–14 May 2004, Rome, Italy
- 21.Operation data furnace 1 from 1-11-2008 to 2-11-2008, AVR Rozenburg, The Netherlands
- 22.Yetter R.A., Dryer F.L. and Rabitz H., " A comprehensive reaction mechanism for carbon monoxide/hydrogen/oxygen kinetics", Combust. Sci. Tech. v79, pp97-128, 1991 J. Austin 6/24/99